Silicon (2021) 13:3473–3497
https://doi.org/10.1007/s12633-020-00792-9

ORIGINAL PAPER

Effect of Nanosilica and Crosslinking System on the Mechanical Properties and Swelling Resistance of EPDM/SBR Nanocomposites with and without TESPT

S. Vishvanathperumal[1] · **G. Anand**[2]

Received: 21 August 2020 / Accepted: 16 October 2020 / Published online: 23 October 2020

Abstract

The ethylene-propylene-diene monomer/styrene-butadiene rubber (EPDM/SBR)-nanosilica (SiO_2) nanocomposite was prepared. The 0–10 parts per hundred rubber (phr) of SiO_2 with EPDM/SBR was mixed on a two-roll mill. The effect of nanosilica (0–10 phr), crosslinking system (sulphur, dicumyl peroxide and mixed) and silane coupling agent (bis(triethoxysilylpropyl)-tetrasulphide) on the curing characteristics, mechanical properties, rebound resilience, compression characteristics, abrasion, swelling property and morphological characteristics of the EPDM/SBR-SiO_2 nanocomposites was investigated and studied. From the results, it was clear that the mechanical, wear and swelling properties steps-up with increase in the content of nanosilica particles in it. The sulphur cured rubber composite exhibits an overall improved properties as compared with other crosslinking agents such as peroxide and mixed systems. The addition of silane coupling agent (SCA) enhances the properties of the nanocomposites to a greater extent. From the analysis, it was clear that the effect of nanosilica concentration in the rubber composite with SCA was found to be superior compared to nanocomposites without it.

Keywords EPDM/SBR · Nanosilica · Crosslinking systems · Silane coupling agent · Mechanical properties

1 Introduction

The introduction of the reinforcement in the rubber matrix improves the properties such as mechanical, physical and thermal properties. At the same time, it also reduces the overall weight and cost of the rubber composites [1, 2]. Currently, more than hundred types of reinforcing materials was used in rubber composite and have been reported in the literatures. But only a few of them are cost-effective, commercialized and extensively used [3]. Carbon black (CB) was commercially used as a reinforcing material in rubber industries in the past decades. The drawbacks associated with the carbon black was its dark colour and pollution related issues. This leads to the development of newer reinforcing materials in the recent decades [4–6] such as montmorillonite [7], silicate layered clays [8], carbon nanotubes [9] and halloysite nanotubes [10] which enhances the mechanical properties, thermal stability and flammability of the rubber composites, when added even in small quantity.

Rice husk was considered as a naturally available agricultural source for the production of nanosilica. The preparation of nanosilica from the rice husk was found to be both environmental friendly and economically beneficial. The major chemical content in the rice husk was the organic materials (such as cellulose and lignin) and silica. Apart from that other minor chemicals found in the rice husk was carbon, nitrogen, oxygen, ferron, sodium, magnesium and aluminum. Generally, this kind of silica was amorphous in nature and will get uniformly dispersed [11] in the rubber material. Most of study in the recent past have confirmed that the silica was used to produce green tires with good mechanical characteristics [12], low rolling resistance [13], and high wet-grip resistance [14] in the rubber matrix [15–17]. But, the presence of more hydroxyl groups on surface of silica material paves a way to

✉ G. Anand
anand.12ng@gmail.com; anand.g@pec.edu

[1] Department of Mechanical Engineering, S.A. Engineering College, Thiruverkadu, Chennai, Tamilnadu 600 077, India

[2] Department of Mechanical Engineering, MVJ College of Engineering, Bangalore, Karnataka 560067, India

the agglomeration of the particle (strong filler-filler interactions), which is lowering the performances of the rubber composites [18–20]. To obtain the high concentration of nanosilica in the rubber matrix with reduced aggregation, in the past numerous research works have been carried out to minimize the hydroxyl groups on surface of silica and to enhance its compatibility between rubber and silica [21]. Moreover, the surface of the silica was high polar in nature which leads to hydrogen bonding with the polar rubber materials, especially amine-based accelerators affects an adsorption of the vulcanizing agents on the silica surface and causes the retardation in the curing reaction [22]. However, the above mentioned disadvantages could be overcome by the use of silica along with silane coupling agent [23, 24].

The blending of the silica particles along with the silane coupling agent (SCA) in rubber mix forces to the chemical reaction called as silanization [25, 26]. It was only the response between the silanol cluster of the silica and the alkoxy cluster of the silane. The discharge mix temperature was the most important parameter considered during the process of silanization [27, 28], where due to the presence of diphenyl guanidine or different amines the reactions are catalyzed [29, 30]. SCA, such as Bis[3-(triethoxysilyl)propyl] tetrasulfide (TESPT), mercaptopropyltriethoxysilane (MEPTS), and bis[γ-triethoxysilylpropyl] disulfide (TESPD), are the commonly used. These materials generally are used for the surface modification of silica particles in the composites [31–33]. The distribution of silica particles in the base material is enhanced by the presence of SCA which reacts with the outer surfaces of the silica particles [34, 35]. The temperature more than 130 °C was the basic requirement for the reactions to take place amongst the base matrix material and silica particles, and in this case TESPT was the commonly used SCA. The SCA at this higher temperature will turn into a sulphur donor that initiates the early curing of SBR [36].

Due to the presence of disulfide bond and high dissociation energy the TESPD are generally stable in nature [37]. Numerous reports in the recent times discusses on the easy dispersal of the silica particles without agglomeration in the base matrix material by surface modification methods by SCA. Phosphonium ionic fluid has additionally been utilized for surface modification of silica particles with the presence of TESPT that enhances the great interfacial interaction amongst the silica particle and SBR matrix [38]. Modification in the surface of the silica particles are done by using different coupling agents by the hydrolysis process to enhance the thermal property of the rubber matrix material. Some of the common coupling agents are γ-chloropropyltrimethoxysilane (CPS), γ-aminopropyltriethoxysilane (APS), and γ-methacryloxypropyltrimethoxysilane (MPS) [39]. The initiator called benzoic peroxide was used for the latex phase grafting of vinyltriethoxysilane (VTEOS) with SBR material [40]. But generally the latex stage process was time consuming, tedious, and less economical one for commercial and industrial applications. Because of that, for the most, melt grafting process was generally usually employed. By reactive blending process, the reactive silane compounds are grafted in the polyethylene matrix material by dicumyl peroxide (DCP) in a Brabender Plastocorder [41]. Banbury mixer was used for the reactive mixing of the TESPD along with the SBR/polybutadiene elastic (BR)/SiO_2 rubber compounds. The reactivity of SCA's with the rubber compounds and their effect on the viscoelastic behavior of the SBR/BR/SiO_2 composite are analyzed [42]. Peroxide initiated grafting of vinyltriethoxysilane and vinyltrimethoxysilane against the polyethylene along with the ethylene propylene copolymer are synthesized and analyzed by using Brabender extruder [43].

The most significant process in rubber compounding that change over the gentle plastic material into an elastomer through forming a 3D – structure is called as Vulcanization. The conventional curing agent such as Sulphur and peroxide are generally used curing the elastomers [44]. Yet still, the peroxide, sulfur and blended curing agents are supposed to have the inflexible C—C bonds, flexible S—S bonds and C—S bonds in general. The rubber blends are the commercially important material for engineering applications as they combine the individual properties of the each rubber compounds in it. Hence these blends are very much beneficial in many industrial applications. It also reduces the overall cost and improves the processability of the final blended rubber compounds [45]. In automotive and constructional applications, amongst the different rubbers, EPDM was generally used, which was a saturated non polar rubber with enhanced ozone, weathering and heat resistant characteristics. But it was associated with a weak adhesive property along with the high cost. Hence to overcome the problems associated with it, the EPDM rubber was mixed with SBR [46].

The EPDM/SBR blend have a wide scope of industrial and commercial application such as conveyer belts, seals, gaskets, tires, tubes and so on [47]. The EPDM/SBR rubber blends with 80/20 proportion have an enhanced mechanical and abrasion characteristics [48]. Hence, the blends are industrially used in various applications. From the literature survey, it is apparent that no appropriate examination have been carried out on the various crosslinking frameworks with SCA alongside with nanosilica particle.

In our previous research work, reported the effect of the nanoclay and crosslinking systems on the mechanical properties and swelling resistance of EPDM/SBR blend nanocomposites. The results showed that the mechanical properties and swelling resistance improved with an increasing content [49]. And then studied the effect of nanoclay/nanosilica content and crosslinking systems on mechanical and swelling properties of EPDM/SBR blend nanocomposites and results revealed that the introduction of nanosilica improved the performance of rubber nanocomposites [50]. Silica has been extensively used as reinforcement in the rubber products, particularly in light-colored rubber products. The current research work was focused on improving the mechanical and swelling properties of EPDM/SBR composite reinforced with nanosilica. The method used for the preparation of rubber composite was melt mixing method in an open mill mixer. The cure characteristics behaviour, mechanical characteristics, rebound resilience, compression behaviour, swelling and abrasion resistance of EPDM/SBR-SiO_2 were studied, with the various concentration of nanosilica (varied from 0 to 10phr). The influences of different crosslinking systems and SCA (bis[3-(triethoxysilyl)propyl]tetrasulfide) on the above mentioned properties of EPDM/SBR-SiO_2 composite was also reported in the paper.

2 Experimental

2.1 Materials

Styrene-butadiene rubber with a styrene concentration of weight percentage 23.5, Mooney viscosity and density of 52 M and 0.93 g/cm^3 was used. The ethylene-propylene-diene rubber with the Mooney viscosity, ethylene termonomer content, and density of 60 M, 68 weight percentage, 4.5%, and 0.86 g/cm^3 respectively was purchased from Arihant Reclamation Pvt. Ltd., was used for the study. The raw rice husk required for the preparation of nano silica was purchased from farmers in Bahour, Puducherry, India and are processed as required. The nanosilica from the raw rice husk was prepared in our laboratory by dissolution and precipitation technique and are stored in a desiccator. The other required chemicals, such as zinc oxide, bis[3-(triethoxysilyl)propyl]tetrasulphide (Si-69), mercaptobenzothiazyl disulphide (MBTS), tetramethylthiuram disulphide (TMTD), peroxide, stearic acid and sulphur of analytically pure and commercial grade was purchased from Vignesh Chemicals, Ambattur, Chennai, India. Sodium hydroxide, sulphuric acid, benzene, toluene, n-octane, dichloromethane, etc., of grade of 99.95% purity was purchased from Sigma Aldrich.

2.2 Preparation of Nanosilica

The raw rice husk from the farmers are collected and are subject to certain process as follows to extract the nano silica from it. The hot plate was used initially to remove the dampness present in the raw rice husk material. Later the treated rice husk was heated above 850 °C for about 7 h in the closed furnace to avoid oxidation and the rice hush ashes are collected from it. The nano silica particles are separated from the rice husk ash by the two stage process namely dissolution and precipitation process. The carbonaceous materials present in the raw rice husk ash are taken away from it by dissolving it in 1 mol of NaOH alkali solution. The final solution (sodium silicate (Na_2SiO_3)) thus obtained were filtered, cleaned and dried for about 30 h at 100 °C in the oven followed by treating the final solution in sulphuric acid for 24 h. During the process the pH should be constantly maintained at 7. Finally the nano silica particles are precipitated through centrifuged process and are washed in hot water and later dried at 75 °C for 20 h [11].

Dissolution Process

$$SiO_2 + 2\,NaOH \rightarrow Na_2SiO_3 + H_2O \tag{1}$$

Precipitation Process

$$Na_2SiO_3 + H_2SO_4 \rightarrow SiO_2 + Na_2SO_4H_2O \tag{2}$$

2.3 Preparation of Composites

The composition of the prepared composites was tabulated in Table 1. Compounding of the material was achieved through an open two-roll mill at the temperature around 80 °C. The different crosslinking systems used are sulphur (S), dicumyl peroxide (DCP) and mixed (S + DCP) and are designated as S, P, and M, respectively, whereas the SCA was represented as T in the study. The composites containing Sulphur as the cross linking material are chosen as S_0 (EPDM/SBR/

Table 1 Formulation for EPDM/SBR-SiO_2 composites

Cross-linking system types	Surface modifier (Si69)	Sample code	Compounds (phr)									
			EPDM	SBR	SiO_2	Si-69	Zinc oxide	Stearic acid	MBTS	TMTD	S	DCP
Sulphur system	Without TESPT	S_0	80	20	0	–	4	1.5	1.2	1	2.5	–
		S_2	80	20	2	–	4	1.5	1.2	1	2.5	–
		S_4	80	20	4	–	4	1.5	1.2	1	2.5	–
		S_6	80	20	6	–	4	1.5	1.2	1	2.5	–
		S_8	80	20	8	–	4	1.5	1.2	1	2.5	–
		S_{10}	80	20	10	–	4	1.5	1.2	1	2.5	–
	With TESPT	ST_0	80	20	0	3	4	1.5	1.2	1	2.5	–
		ST_2	80	20	2	3	4	1.5	1.2	1	2.5	–
		ST_4	80	20	4	3	4	1.5	1.2	1	2.5	–
		ST_6	80	20	6	3	4	1.5	1.2	1	2.5	–
		ST_8	80	20	8	3	4	1.5	1.2	1	2.5	–
		ST_{10}	80	20	10	3	4	1.5	1.2	1	2.5	–
Peroxide system	Without TESPT	P_0	80	20	0	–	–	–	–	–	–	4
		P_2	80	20	2	–	–	–	–	–	–	4
		P_4	80	20	4	–	–	–	–	–	–	4
		P_6	80	20	6	–	–	–	–	–	–	4
		P_8	80	20	8	–	–	–	–	–	–	4
		P_{10}	80	20	10	–	–	–	–	–	–	4
	With TESPT	PT_0	80	20	0	3	–	–	–	–	–	4
		PT_2	80	20	2	3	–	–	–	–	–	4
		PT_4	80	20	4	3	–	–	–	–	–	4
		PT_6	80	20	6	3	–	–	–	–	–	4
		PT_8	80	20	8	3	–	–	–	–	–	4
		PT_{10}	80	20	10	3	–	–	–	–	–	4
Mixed system	Without TESPT	M_0	80	20	0	–	4	1.5	1.2	1	2.5	4
		M_2	80	20	2	–	4	1.5	1.2	1	2.5	4
		M_4	80	20	4	–	4	1.5	1.2	1	2.5	4
		M_6	80	20	6	–	4	1.5	1.2	1	2.5	4
		M_8	80	20	8	–	4	1.5	1.2	1	2.5	4
		M_{10}	80	20	10	–	4	1.5	1.2	1	2.5	4
	With TESPT	MT_0	80	20	0	3	4	1.5	1.2	1	2.5	4
		MT_2	80	20	2	3	4	1.5	1.2	1	2.5	4
		MT_4	80	20	4	3	4	1.5	1.2	1	2.5	4
		MT_6	80	20	6	3	4	1.5	1.2	1	2.5	4
		MT_8	80	20	8	3	4	1.5	1.2	1	2.5	4
		MT_{10}	80	20	10	3	4	1.5	1.2	1	2.5	4

SiO_2 80/20/0), S_2 (EPDM/SBR/SiO_2 80/20/2), S_4 (EPDM/SBR/SiO_2 80/20/4) and so on. Whereas the composites containing silane coupling agent are designated as ST_0 (EPDM/SBR/SiO_2/TESPT 80/20/0/3), ST_2 (EPDM/SBR/SiO_2/TESPT 80/20/2/3), ST_4 (EPDM/SBR/SiO_2/TESPT 80/20/4/3) and similarly. The rubber composites which contains peroxide and mixed systems are chosen as P_0 and M_0 (EPDM/SBR/SiO_2 80/20/0), P_2 and M_2 (EPDM/SBR/SiO_2 80/20/2), P_4 and M_4 (EPDM/SBR/SiO_2 80/20/4), etc., and same composites containing silane coupling agent are designated as PT_0 and MT_0 (EPDM/SBR/SiO_2/TESPT 80/20/0/3), PT_2 and

MT_2 (EPDM/SBR/SiO_2/TESPT 80/20/2/3), PT_4 and MT_4 (EPDM/SBR/SiO_2/TESPT 80/20/4/3) and so on. The subscripts indicate the content of nanosilica in the composites. EPDM was masticated and blended with SBR and then nanosilica, Si-69 and curatives were added to it. Finally, 10 end-roll passes was made before making it into sheets. The compounded rubber was left for around 24 h idle before the vulcanization process. The process was done in semi-automated hydraulic press at a temperature and pressure of 160 °C and 30 MPa respectively at the optimal time period. The designated compound rubber sheet of 15 cm × 15 cm × 0.2 cm sizes was made during the process.

2.4 Characterization

2.4.1 Rheometric Characteristic

The cure behavior of the unvulcanized rubber compounds for the different conditions are analyzed by using an oscillating disc rheometer, at the standard operating condition of 160 °C, oscillation arc 0.5^o and 100 cycles per minutes as per ASTM D-2084. The CRI of the rubber compound was determined using the eq. (3):

$$CRI = \frac{100}{Optimum\ cure\ time - Scorch\ time} \tag{3}$$

Where, CRI = Cure Rate Index.

2.4.2 Mechanical Properties

The tensile property of the composite was analyzed in the universal tensile machine of make and model: series 7200, Dak System Inc. and T-72102 as per ASTM D-412. The crosshead speed of the tensile test machine was maintained at 500 mm/min [51, 52]. Dumb-bell shaped specimens (using type-C die) and un-nicked 90^o angle test-shaped specimens (using type-B die) was prepared and the tensile and tear properties are

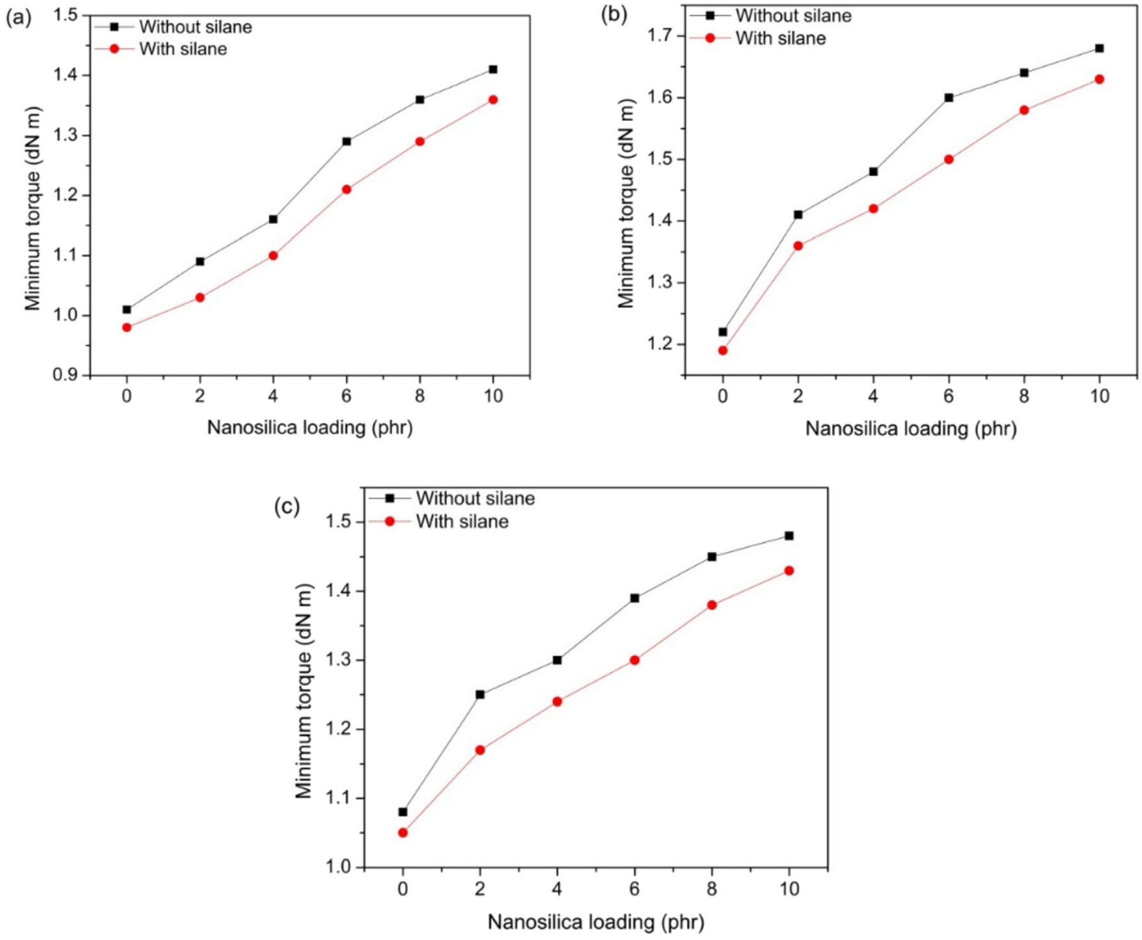

Fig. 1 Minimum torque of the EPDM/SBR composites: **a** Sulphur cured composite, **b** Peroxide cured composite and **c** Mixed system cured composite

analyzed. The tear characteristics are also performed in the same machine as per ASTM D-624. The average of five samples values are taken for each composite composition and are tabulated and analyzed. Shore – A Durometer was used to determine the hardness of the rubber compounds as per ASTM D-2240 procedure.

2.4.3 Swelling Properties

The rubber composite samples are used to analysis the swelling characteristics as per ASTM D-471 through immersion technique. Different solvents such as aromatic, aliphatic and chlorinated hydrocarbons (Benzene, n-heptane, carbon tetrachloride, etc.,) are used to analysis the swelling characteristics of the rubber blend at a constant temperature of 30 °C. The initial and final weight of the samples are measured by using a precision weighing machine at periodic time period and the process continues up to equilibrium swelling point. The results are plotted against the time and mole percent uptake (Q_t). The mole percent uptake was determined using the Eq. (4) below:

$$Q_t(mol\%) = \frac{(M_t - M_0)/MW}{M_0} \times 100 \tag{4}$$

where, M_t = Mass after the time of 72 h of immersion, M_0 = Compounds initial mass, MW = Solvents molecular weight.

2.4.4 Crosslinking Density

The degree of crosslinking density of the composite materials was determined using the formulae (5) [53–55]:

$$\vartheta\left(\frac{mol}{cm^3}\right) = \frac{1}{2M_c} \tag{5}$$

where M_c = molar mass of the polymer between crosslinks and it can be determined using the following Eq. (6) [53–56]:

$$M_c\left(\frac{g}{mol}\right) = \frac{-\rho_p V_s V_r^{1/3}}{\ln(1-V_r) + V_r + \chi V_r^2} \tag{6}$$

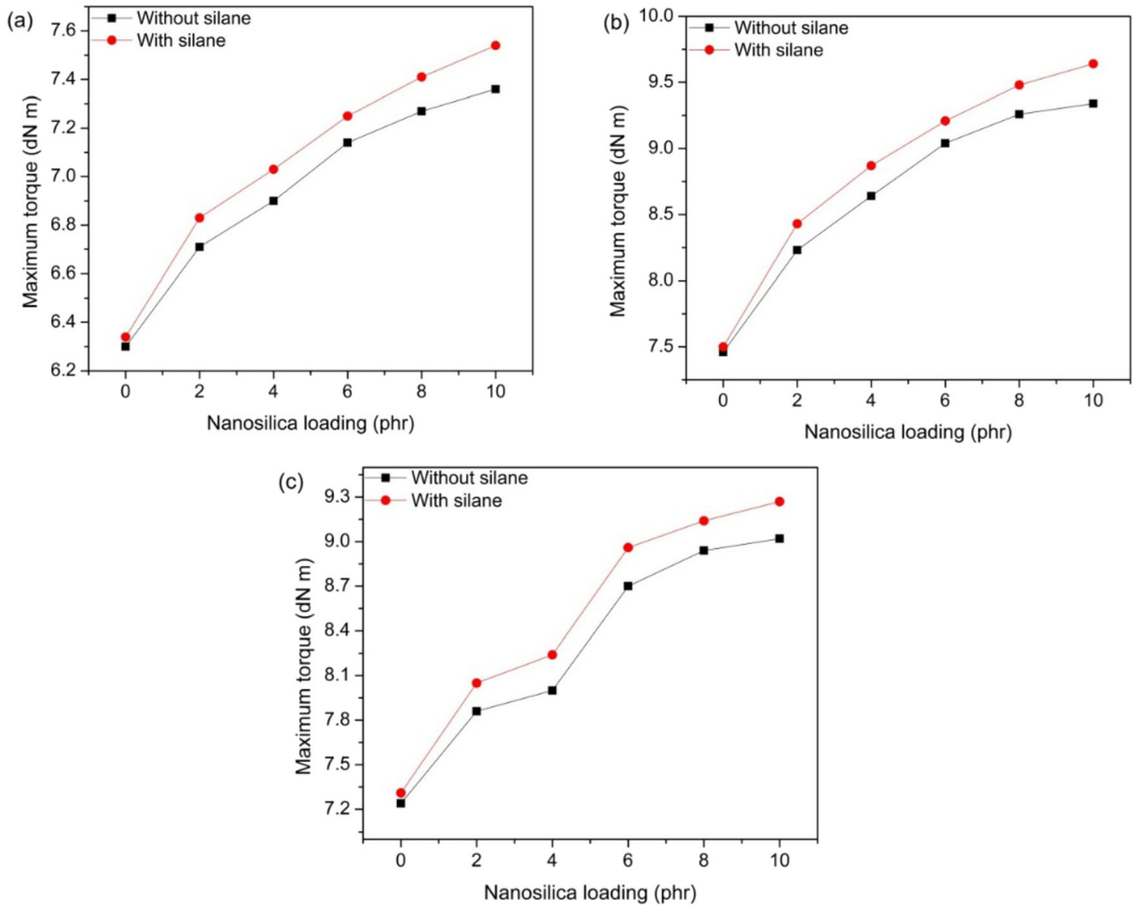

Fig. 2 Maximum torque of the EPDM/SBR composites: **a** Sulphur cured composite, **b** Peroxide cured composite and **c** Mixed system cured composite

where, ρ_p = polymer density, V_s = Solvent molar volume (106.3 mL/gmol), V_r = Volume fraction of solvent-swollen filled rubber compound, χ = Constant parameter for polymer interaction (0.3) [57], Hence V_r can be determined using the following Eq. (7) [58]:

$$V_r = \frac{1}{1 + Q_m} \tag{7}$$

where, Q_m = Composite weight swell in toluene.

2.4.5 Rebound Resilience

The characteristics of the rebound resilience of the blended rubber compounds was determined in the vertical rebound tester called resiliometer (ASTM D-2632). In this technique, the rebound height of the plunger was measured when suspended from a predetermined height. The ratio between the two height of the plunger represents the value of the rebound resilience. In general, it will be expressed in percentage.

2.4.6 Abrasion Resistance

Abrasion characteristics of the composite material was determined as per ASTM D-5963 on Zwick Abrasion tester - DIN abrader - model 6102 and are generally expressed in terms of loss in the volume ratio. The composite specimen of the respective dimension was abraded through a grade 60 sandpaper with a constant force and speed of 10 N and 0.32 m/s respectively for about 40 m. For each specimen average of 5 samples are considered. The wear loss in the rubber composite was determined using the Eq. (8):

$$Abrasion\ loss\ \left(mm^3\right) = \frac{\Delta m \times S_0}{\rho \times S} \tag{8}$$

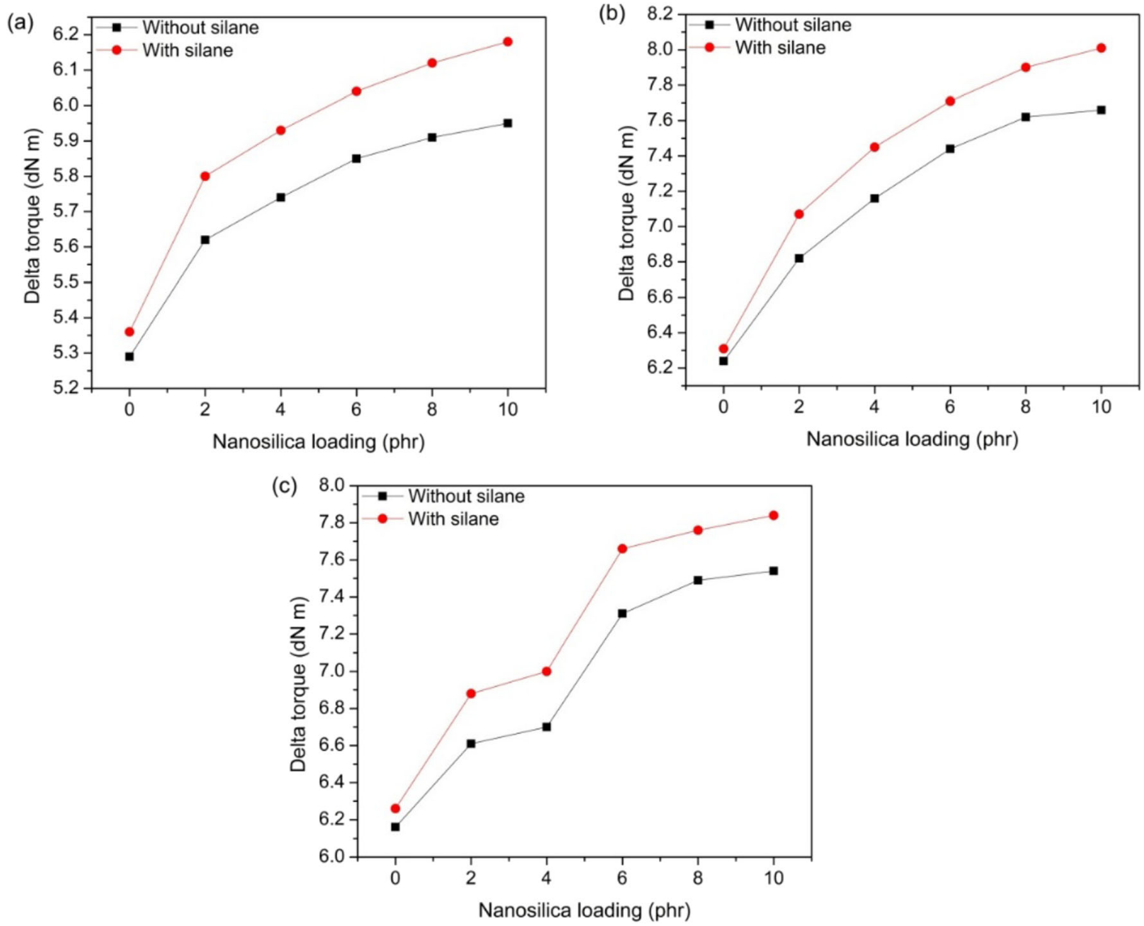

Fig. 3 Delta torque of the EPDM/SBR composites: **a** Sulphur cured composite, **b** Peroxide cured composite and **(c)** Mixed system cured composite

where, Δm = mass loss in mg; ρ = density in mg/mm^3; S_0 = value of nominal abrasive power for 200 mg; S = average abrasive power in mg.

2.4.7 Compression Set

The compression set characteristics of the rubber composite sample was done as per ASTM D-395. The digital vernier caliper with an accuracy of 0.01 mm was used to measure the initial and final thickness of the sample which is compressed at 25% deflection. The test was performed at the room temperature of 23 °C for 24, 48 and 72 h respectively and are placed in an air circulated oven at a temperature of 70 °C and 100 °C for 24 h. The compression set values of the composite samples are obtained using the following Eq. (9):

$$Percentage\ of\ compression\ set, C\% = \frac{t_0 - t_1}{t_0 - t_s} \times 100 \tag{9}$$

where, t_0 = Original thickness of the specimen, t_1 = Final specimen thickness and t_s = Spacer bar thickness.

2.4.8 Morphology

The fractured surface of the rubber composite samples are examined by means of field emission scanning electron microscopy (FESEM) of make and model Hitachi S-4160. The surface to be analyzed are coated with gold layer to make it conductive in nature. The samples are analyzed under the accelerating voltage of about 3 kV in general.

3 Results and Discussion

3.1 Rheometric Characteristic

The rheometric characteristics of a compound was greatly influenced by the presence of type of filler component in it, its type and concentration [8] and its surface property [59]. Figures 1, 2, 3, 4, 5 and 6 presents the cure characteristics behaviour of the rubber blend composite reinforced with SiO_2 at various concentrations, as

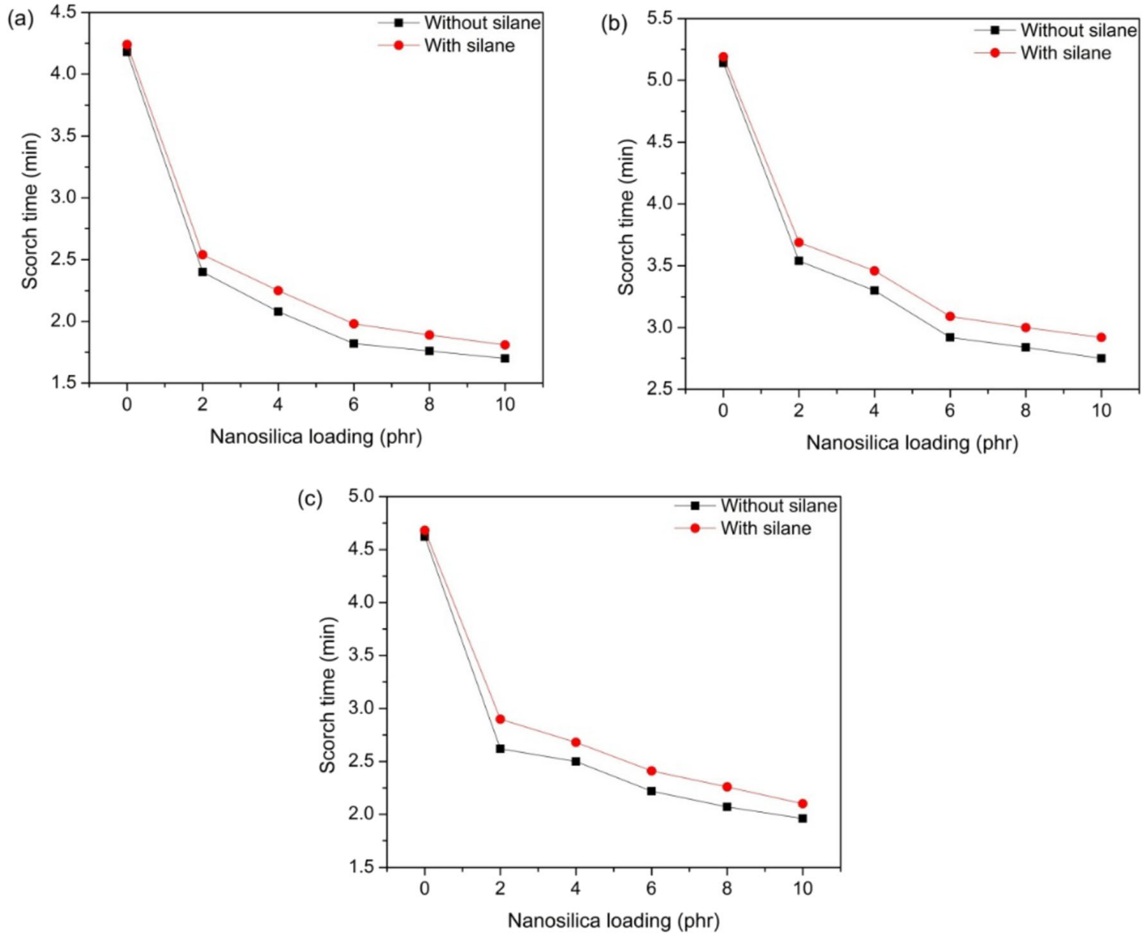

Fig. 4 Scorch time of the EPDM/SBR composites: **a** Sulphur cured composite, **b** Peroxide cured composite and **(c)** Mixed system cured composite

functions of silica nanoparticles, silane coupling agent and crosslinking systems. The different rheometric characteristics such as minimum torque (M_l), maximum torque (M_h), delta torque (ΔM), scorch time (t_{s2}), optimum cure time (t_{c90}) and cure rate index (CRI) are analyzed and examined in detail.

At the constant temperature, the viscosity of the rubber blends and the minimum torque are directly interconnected to it. Hence the viscosity of the masticated rubber (unvulcanized rubber) is calculated in terms of it [8]. The Fig. 1, shows the minimum torque of composites. The incorporation of the silica nanoparticle in the blended rubber composite results in increase in the minimum torque, because at higher concentration of nanosilica the viscosity of the EPDM/SBR composite was increased. Comparing different crosslinking system cured EPDM/SBR composites with and without silane coupling agent (TESPT), the minimum torque thus obtained was similar. The peroxide cured EPDM/SBR composites without TESPT showed an increase in viscosity as they incorporated the highest amount of nanosilica in it. Minimum torque are higher in composites vulcanized with peroxide. This may be due to its ability to promote the curing of rubber compounds and also because of the structure of crosslinks developed during the curing time with peroxide, which was considered by rigid carbon – carbon bonds and stable bonds. The composites with TESPT exhibited lower minimum torque which indicates the better processability as compared to the composites without TESPT.

The maximum torque may be interconnected as the measure of stock modulus. Figure 2, shows the maximum torque of rubber blend composites. The nanosilica loaded EPDM/SBR composites with and without TESPT indicates a maximum torque with increases in the percentage of nanosilica and this remains same for all the crosslinking system. The mobility of the rubber chain in the composite reduces with increase in the presence of nanosilica and thus increases its maximum torque. Nanosilica filled EPDM/SBR composites with TESPT exhibits a higher of maximum torque as compared to the composites without TESPT. The improvement in

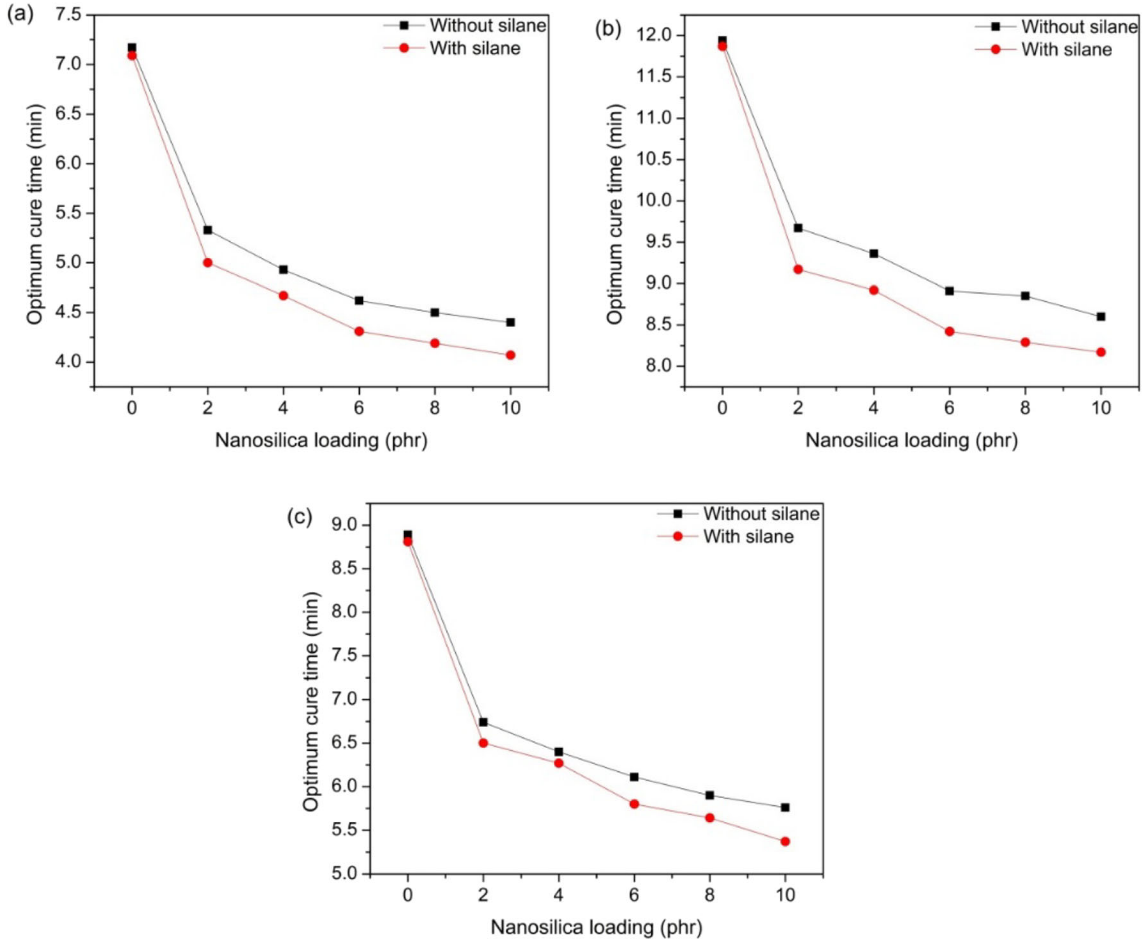

Fig. 5 Optimum cure time of the EPDM/SBR composites: **a** Sulphur cured composite, **b** Peroxide cured composite and **c** Mixed system cured composite

maximum torque was because of the greater interaction among the nanosilica and EPDM/SBR blend especially with existence of TESPT in it. The addition of TESPT in the peroxide cured EPDM/SBR results in an increase of maximum torque, showing a considerable increase of the crosslink degree.

Furthermore, the cure characteristics represents several physical parameters that state to the microstructural behavior of the rubber blends. The delta torque was a secondary suggestion of the degree of crosslinking of the rubber composites. Figure 3 indicates the delta torque of composites. Crosslinking density was determined from the eq. 5 which corresponds with the deviation in the delta torque. Delta torque gradually steps up with increasing in the percentage of nanosilica for all the curing system. The delta torque increased as the plasticizer effect decreased, due to decreased slippage between the rubber chains occurs as the crosslinking density is increased. The delta torque for the composites filled with higher content of nanosilca particles are higher than unfilled blends, indicating that the crosslinking between the rubber matrix and silica and the interaction at the nanosilica particles-rubber matrix interface are higher in the case of the higher amount of nanosilica filled composites [60]. The peroxide cured EPDM/SBR with TESPT showed an increase in viscosity as they incorporated the highest amount of nanosilica. Peroxide promotes the curing of the EPDM/SBR composites, as expected. On the other hand, the addition of TESPT in the EPDM/SBR-nanosilica composites resulted in a complete suppression, shows that the primary free radicals originated from peroxide were consumed by the TESPT.

The premature vulcanization in the composite was measured by scorch. Figure 4 presents the scorch time of composites. For different crosslinking system cured EPDM/SBR composites with and without TESPT, it was seen that the incorporated nanosilica reduced the scorch time. The sulphur cured EPDM/SBR composite exhibited the lowest values for scorch time. As a result, the addition of nanosilica accelerated the curing process more efficient than peroxide cured one. The

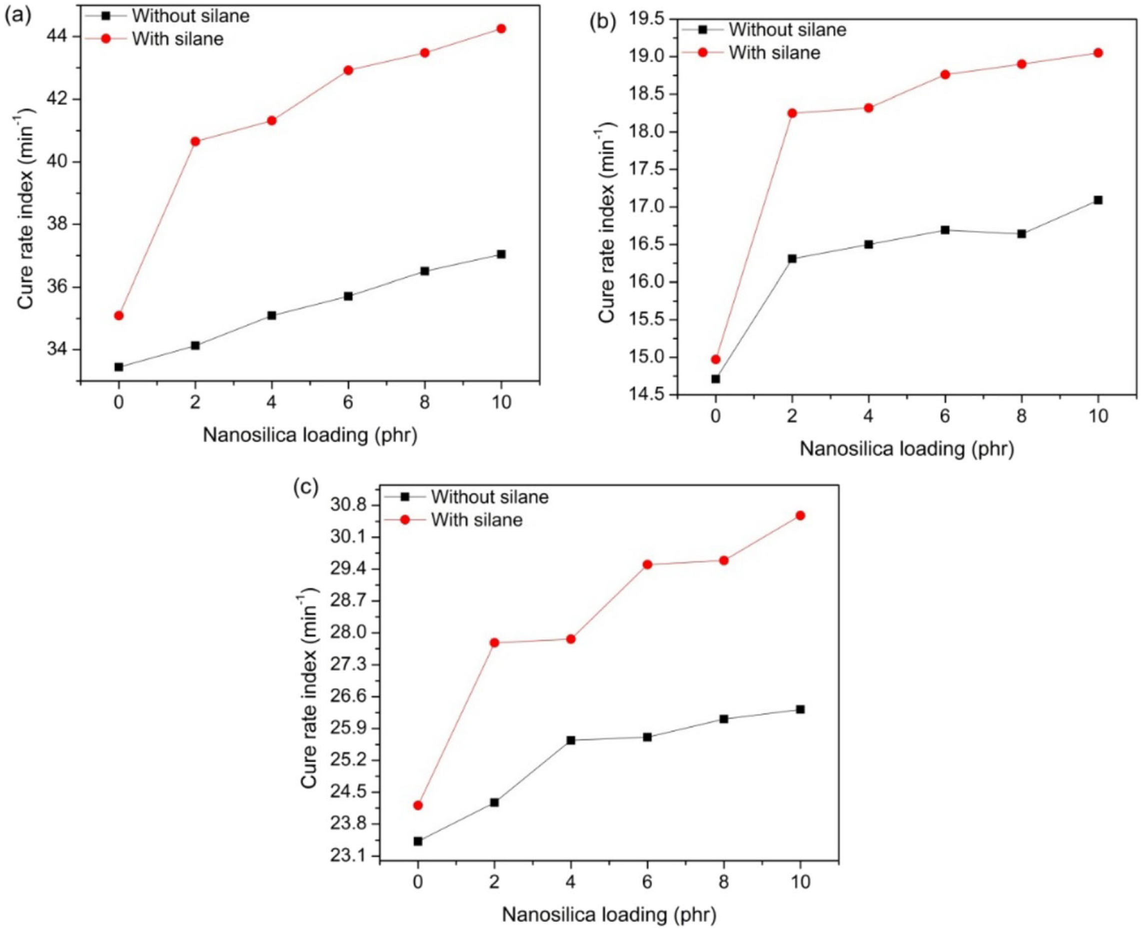

Fig. 6 Cure rate index of the EPDM/SBR composites: **a** Sulphur cured composite, **b** Peroxide cured composite and **c** Mixed system cured composite

scorch time shows that the adsorption of curatives by nanosilica consequences in the delayed scorch time in EPDM/SBR composite with TESPT. From the analysis it is also clear that the TESPT induced composite have an enhance growth in scorch time in par with the composite without TESPT. This is due to the uniform dispersion of nanosilica particles and TESPT. Higher scorch time shows that composites with nanosilica particles and TESPT has better processability [24].

The optimum cure time was a measure of the minimum time required to meet the maximum torque of about 90%. It is used to measure the time for complete curing of the rubber compound. Figure 5 clearly indicates the optimum cure time of the rubber blend composites. For different crosslinking system cured EPDM/SBR composites with and without TESPT, it was seen that the incorporated nanosilica reduced the optimum cure time. The sulphur cured EPDM/SBR composite exhibited the lowest values for optimum cure time. For sulphur cured composites, the reactive species formed rapidly and curing process started almost two times faster than in the peroxide cured one. The optimum cure time of composites filled with nanosilica particles and TESPT is slightly lower compared to the similar composite with silica nanoparticles. After introduction of TESPT, the number of silanol groups (-OH) on silica surface reduced and as a result decreased the optimum cure time in the vulcanization process [24]. EPDM/SBR with high nanosilica loading and TESPT showed a reduction in optimum cure time of about 43%.

The cure rate index (CRI) of composites was clearly represented in Fig. 6. The CRI increases with increasing content of nanosilica. The increase in the CRI indicates the maximum rate of curing and are attributed to the presence of nanosilica and crosslinking agent in EPDM/SBR composites. Due to which there is a considerable increase in the curing rate of the rubber blend composite. The sulphur cured EPDM/SBR composite exhibited the highest for cure rate index. This effect is affected by the rigidity of

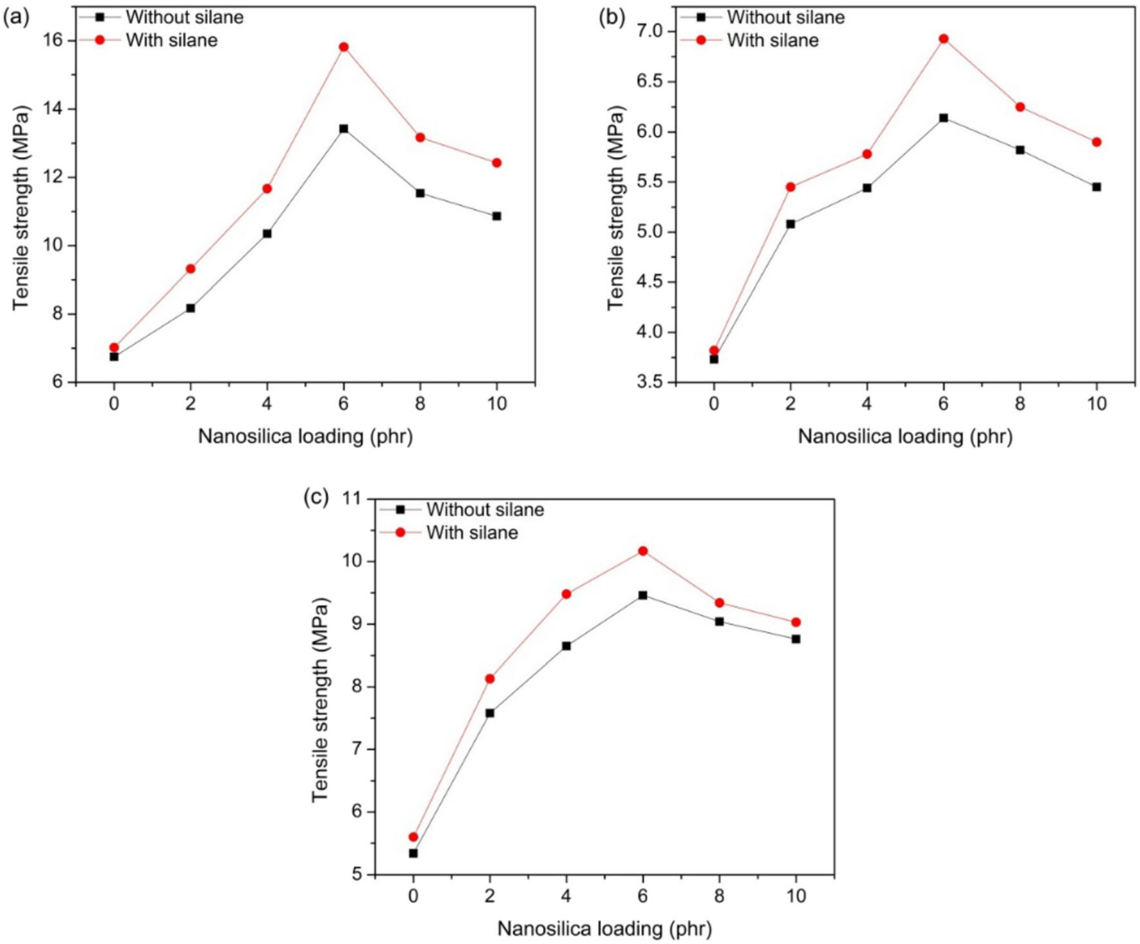

Fig. 7 Tensile strength of the EPDM/SBR composites: **a** Sulphur cured composite, **b** Peroxide cured composite and **c** Mixed system cured composite

nanosilica. Overall, the curing characteristics of the EPDM/SBR composites revealed that nanosilica acted as reinforcing filler. The addition of the nanosilica and constant TESPT with different crosslinking system increased torque and decreased times compared to the neat EPDM/SBR composite.

3.2 Mechanical Properties

The mechanical characteristics of the EPDM/SBR-SiO_2 composites were investigated by comparison with neat different crosslinking system cured EPDM/SBR composite with and without TESPT. The tensile strength of different crosslinking cured rubber blend composites with respect to the concentration of nanosilica and TESPT is represented in Fig. 7, similarly for 100% modulus and elongation at break it is represented in Figs. 8 and 9. The tensile strength, 100% modulus and elongation at break of EPDM/SBR composites steps up with positive loading of nanosilica up to 6phr and then steps down gradually for all the system, which can be due to the crosslink density as represented in Fig. 10. This indicating nanosilica was an effective in improving the tensile properties of EPDM/SBR composites.

For sulphur cured system, compared with neat EPDM/SBR, incorporation of 6 phr of nanosilica resulted in a roughly 99% increase in tensile strength, from 6.75 MPa to 13.43 MPa, 100% modulus increased by 44% and the elongation at break increased by 22%, while for neat EPDM/SBR with TESPT, addition of 6 phr of nanosilica resulted in a nearly 125% increase in the tensile strength, from 7.02 MPa to 15.82 MPa, 100% modulus increased by 47% and the elongation at break increased by 19%, indicating of reinforcing and toughening effects of nanosilica on EPDM/SBR matrix. From the analysis of tensile strength, it is clear that the presence of TESPT can increase the dispersion capability of the silica nanoparticles and its interfacial interaction with EPDM/SBR matrix blend. Similarly, for peroxide cured system, compared with neat EPDM/SBR, incorporation of 6 phr of nanosilica

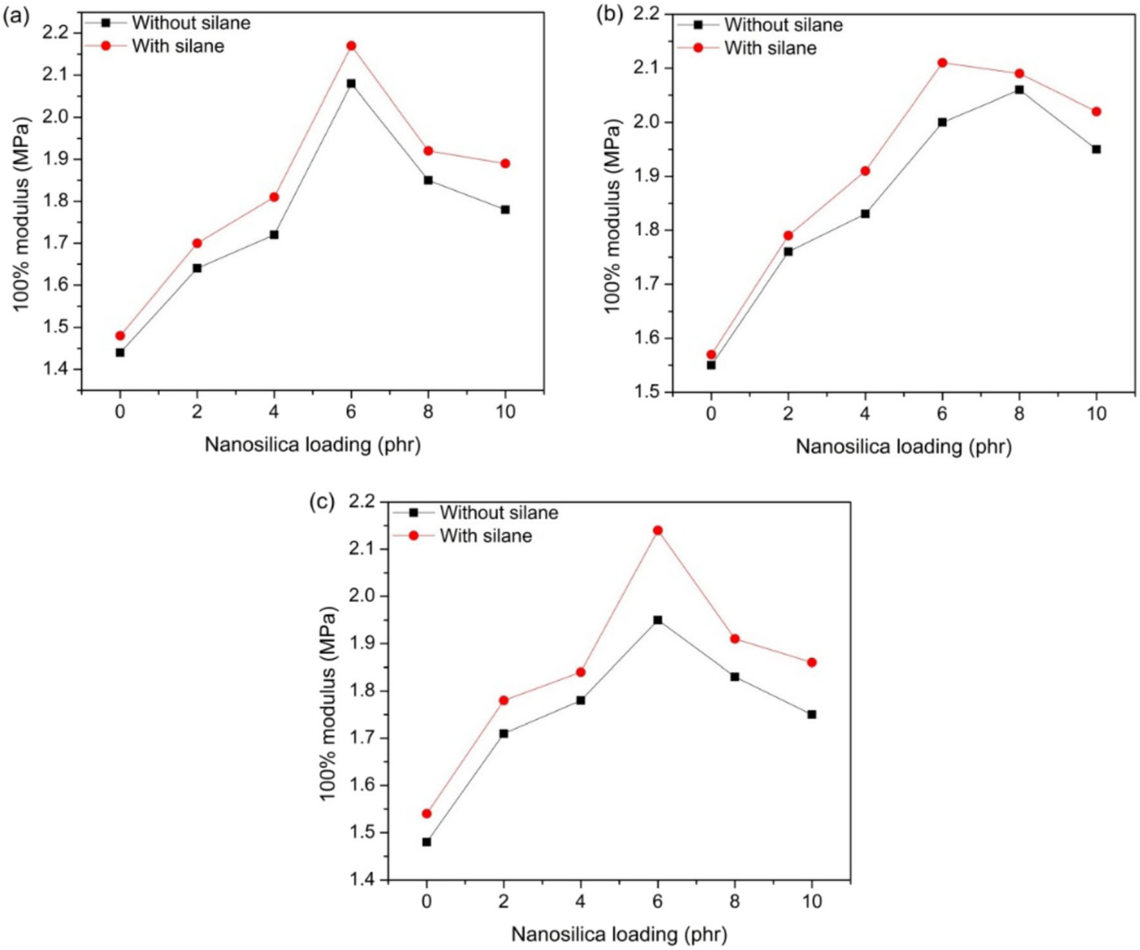

Fig. 8 100% modulus of the EPDM/SBR composites: **a** Sulphur cured composite, **b** Peroxide cured composite and **c** Mixed system cured composite

resulted in a roughly 65% increase in tensile strength, from 3.73 MPa to 6.14 MPa, 100% modulus increased by 29% and the elongation at break increased by 23%, while for neat EPDM/SBR with TESPT, addition of 6 phr of nanosilica resulted in a nearly 81% increase in the tensile strength, from 3.82 MPa to 6.93 MPa, 100% modulus increased by 34% and the elongation at break increased by 21%, indicating of reinforcing and toughening effects of nanosilica on EPDM/SBR matrix. Similarly, for mixed (sulphur and peroxide) cured system, compared with neat EPDM/SBR, incorporation of 6 phr of nanosilica resulted in a roughly 77% increase in tensile strength, from 5.34 MPa to 9.46 MPa, 100% modulus increased by 32% and the elongation at break increased by 27%, while for neat EPDM/SBR with TESPT, addition of 6 phr of nanosilica resulted in a nearly 82% increase in the tensile strength, from 5.6 MPa to 10.17 MPa, 100% modulus increased by 39%, and the elongation at break increased by 24%, indicating of reinforcing and toughening effects of nanosilica on EPDM/SBR matrix. Such trend is frequently observed in rubber composites with increasing crosslink density. Figure 7 shows that the tensile strength of the rubber blend composites with TESPT. The Presence of TESPT clearly improve its tensile strength and thus improves an interaction among silica nanoparticles and rubber blends by the coupling reaction of the silane. As for 6 phr of nanosilica particles filled composites, the tensile strength value is the highest, indicating the better dispersion of nanosilica particles in the rubber matrix. This result is in good evident with the FESEM images [23]. Sulphur cured composites with TESPT shows better result than that of composites without TESPT. The interaction among the nanosilica particles and the rubber blends by silane, which improves the tensile strength of the rubber blend composites, reduces its elongation at break, as represents in Fig. 8. This is due to ethoxy-group present to react with the hydroxyl group of surface of nanosilica, leading to better dispersal of nanosilica particles in the rubber blend. 100% modulus is also showed a similar trend, as shown in Fig. 9.

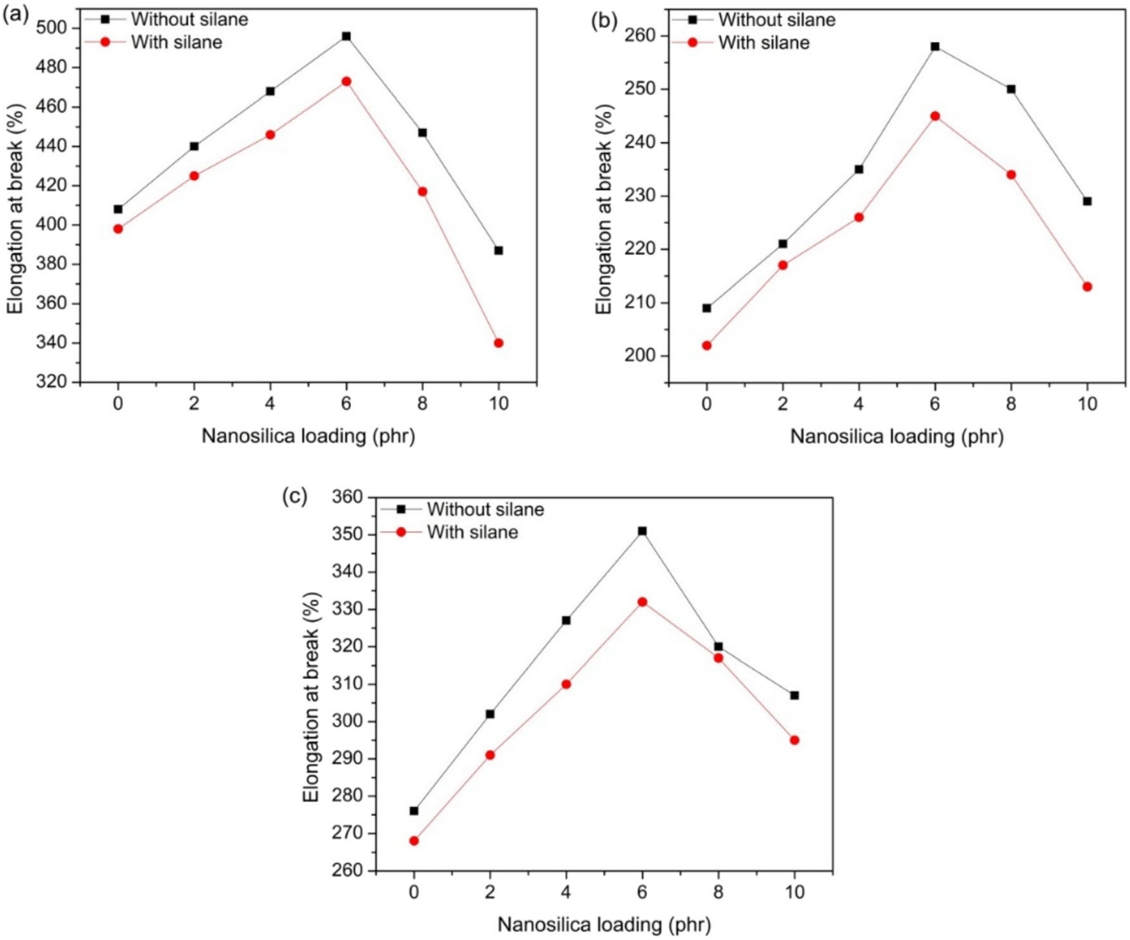

Fig. 9 Elongation at break of the EPDM/SBR composites: **a** Sulphur cured composite, **b** Peroxide cured composite and **c** Mixed system cured composite

The influence of nanosilica percentage on the tear property of the different crosslinking system cured EPDM/SBR composite with and without TESPT is represented in Fig. 11. For all the curing system, the tear strength of the prepared rubber blend composites was found to steps up with an increase in the percentage of nanosilica content. The sulphur cured system with and without TESPT shows the better tear strength as compared to the composite with other two system. The sulphur cured system shows higher tear strength due to the flexible sulphur – sulphur (S - S) bonds. From the Fig. 11, the tear property of silica nanoparticles filled composites are obviously increased compared with unfilled blends, mainly due to the hydroxyl groups on the surface of nanosilica particles react with TESPT. As for highly silica nanoparticles filled composites, the tear property value is the highest, indicating the good dispersion of silica nanoparticles in the rubber matrix [23]. EPDM/SBR composite filled with nanosilica and TESPT shows increased tear strength arising out of increased cross-linking density and better nanosilica dispersion [61].

The effect of nanosilica concentration with respect to the hardness characteristics for the different crosslinking system with and without TESPT is represented in Fig. 12. The hardness of EPDM/SBR composites steps up with increase in the percentage of nanosilica content in it for all the systems. It is observed that at similar composite ratio, the hardness of EPDM/SBR composites with TESPT is found to be as compared to the composite without TESPT, in specific at higher concentration of nanosilica. This improvement in the hardness shows that proper wetting of nanosilica particles and stronger rubber-filler interfacial adhesion [24]. A stable Si-O-Si bond is observed between the silane and the nanosilica surface, when TESPT was used [62]. Higher crosslinking density plays major role in determining the maximum hardness. As the crosslinking density is increased, the hardness property of composites increases with

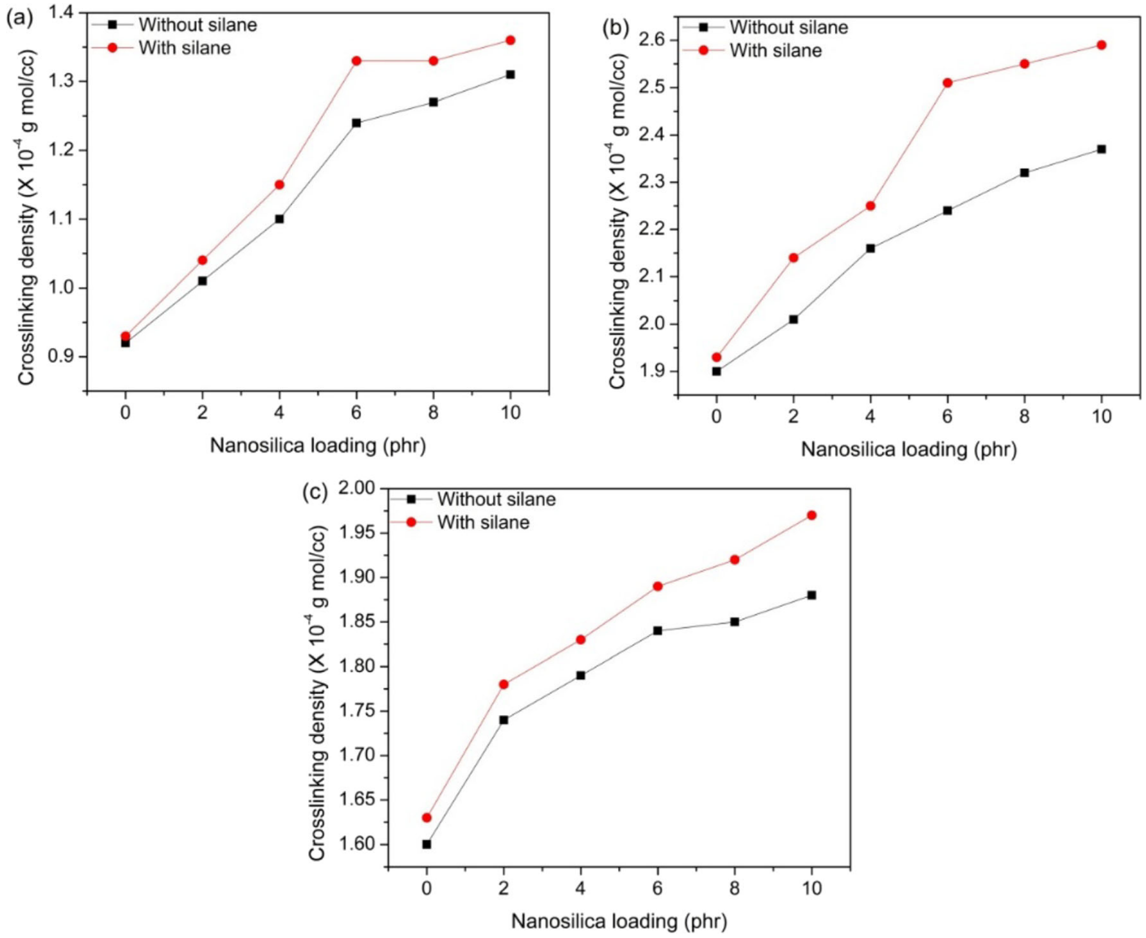

Fig. 10 Crosslinking density of the EPDM/SBR composites: **a** Sulphur cured composite, **b** Peroxide cured composite and **c** Mixed system cured composite

the presence of TESPT in part to the composites without the presence TESPT, hence there is an increase in the crosslinking density in the composite. As the crosslinking density steps up, the soft rubber material becomes harder. As compare to the three different curing system, peroxide system gives a better hardness to EPDM/SBR composite.

3.3 Swelling Properties

The effects of different parameters such as nanosilica loading, crosslinking systems, type of solvents, etc., on mole percent uptake in the rubber blend composites are analyzed. The swelling characteristics of the rubber blend composite mainly subjected to the free volume, the polymeric chains mobility, penetrants and the molecular size of the solvent used. Tables 2, 3 and 4 show the comparison for mole percent uptake of aliphatic, chlorinated, and aromatic solvents by rubber blend - SiO_2 composites with and without TESPT crosslinked by different crosslinking system.

Figure 13 shows the mole percent absorption of benzene by content of nanosilica crosslinked with sulphur. Similar to unfilled EPDM / SBR blends, the absorption of benzene solvent is reduced for the nanosilica packed EPDM / SBR composites. The graph clearly shows that the neat rubber has the highest uptake of equilibrium, and the addition of nanosilica in the neat rubber frequently reduces the uptake of the mole per cent. The introduction of nanosilica has decreased the number of free spaces in the EPDM / SBR blend matrix, limited segmental mobility of the EPDM / SBR blend matrix, and creates the tortuous path for swelling solvent molecules through the EPDM / SBR composites. The same trend with different solvents was observed, as shown in Tables 2, 3, 4.

The mole percent uptake of toluene through EPDM/SBR composites crosslinked with different crosslinking systems was seen in Fig. 14. Figure 14 clearly indicated that the peroxide cured composites absorb the lowest degree of solvent, mixed system cured composites taking on the intermediate behavior

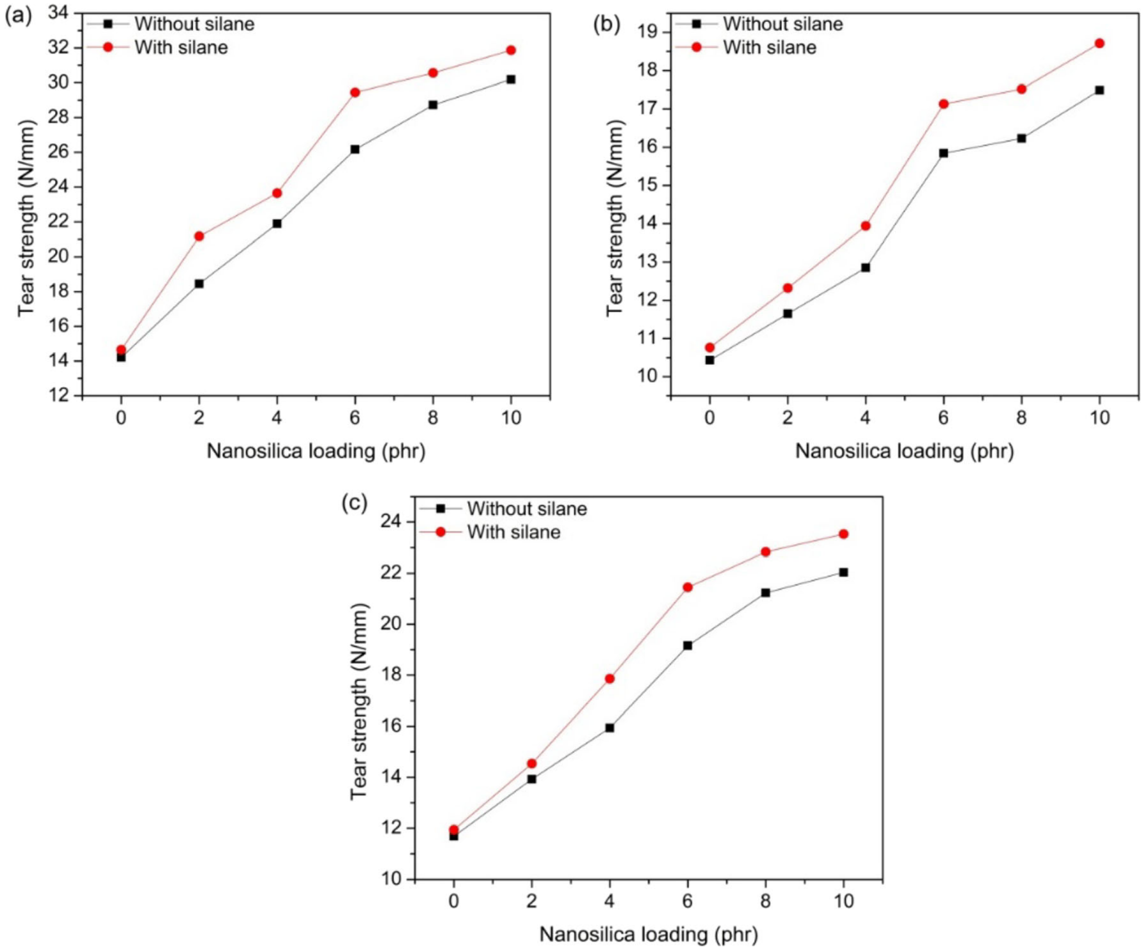

Fig. 11 Tear strength of the EPDM/SBR composites: **a** Sulphur cured composite, **b** Peroxide cured composite and **c** Mixed system cured composite

while sulphur cured composites absorb the highest amount of solvent. The disparity in the intake of composites with different cross-linking systems (sulphur, peroxide and mixed) may be due to the development of various forms of crosslinks between rubber chains during the curing process [63, 64]. The same trend was observed with different solvents as shown in Tables 2, 3, 4.

Figure 15 showed the impact of penetrating size on the mole's percent absorption of various aliphatic solvents (i.e., n-pentane, n-hexane, n-heptane and n-octane) by 10 phr nanosilica filled EPDM / SBR composites crosslinked with peroxide. It was clear from Fig. 15 that the trend was in the order of: pentane > hexane > heptane > n-octane. The solvent molecule's high molecular weight exhibited the lowest absorption while the solvent molecule's low molecular weight exhibited the highest absorption. The molecular mass and solvent are usually in inverse relation. The same pattern has been observed for various solvents as shown in Tables 2, 3, 4.

Figure 16 shows the impact of TESPT on the mole percent absorption of chlorinated solvents (i.e., dichloromethane, chloroform, and carbon tetrachloride) by 10-phr nanosilica-filled EPDM / SBR composites crosslinked with mixed systems. It was observed that all composites (with and without TESPT) exhibited the same pattern, where the mole percent uptake decreased as nanosilica content increased. The findings were attributed primarily to the composites being incompatible. Nanosilica forms a strong hydrogen bond since its surface was acidic, as a result it would reduce solvent resistance. However, with the addition of TESPT in nanosilica filled EPDM/SBR composites, the solvent resistance was improved to a greater extent. The swelling resistance of nanosilica-filled EPDM / SBR composites with TESPT was higher than without TESPT, can be seen at a similar composite ratio. When using TESPT a strong Si-O - Si bond was formed between the surface of the silane and the surface of the silica nanoparticle. The

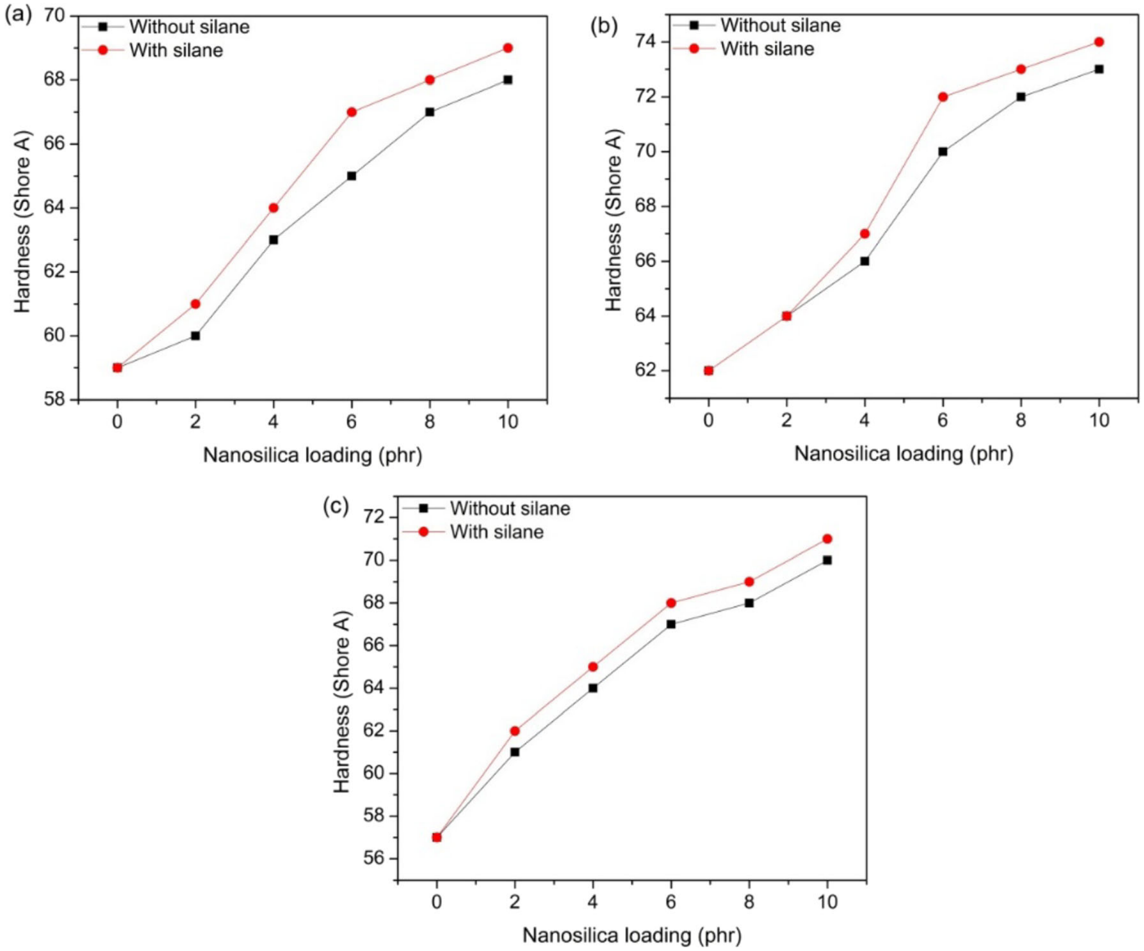

Fig. 12 Hardness of the EPDM/SBR composites: **a** Sulphur cured composite, **b** Peroxide cured composite and **c** Mixed system cured composite

Table 2 Mole percent uptake of aromatic penetrant of EPDM/SBR-SiO_2 composites with and without TESPT

Crosslinking system types	Nanosilica loading	Mole percent uptake (mol%) of aromatic penetrant							
		Without TESPT				With TESPT			
		Benzene	Toluene	Xylene	Mesitylene	Benzene	Toluene	Xylene	Mesitylene
Sulphur system	0	3.95	3.57	3.46	3.03	3.92	3.54	3.44	3
	2	3.7	3.34	3.23	2.9	3.61	3.27	3.15	2.82
	4	3.57	3.14	3.04	2.78	3.52	3.05	2.97	2.66
	6	3.4	2.9	2.76	2.65	3.28	2.77	2.59	2.5
	8	3.33	2.84	2.7	2.6	3.23	2.75	2.55	2.46
	10	3.3	2.78	2.66	2.55	3.19	2.71	2.52	2.41
Peroxide system	0	2.58	2.27	2.07	2	2.55	2.25	2.04	1.97
	2	2.35	2.17	1.8	1.82	2.28	2.08	1.72	1.66
	4	2.24	2.06	1.78	1.76	2.17	2	1.65	1.6
	6	2.17	2	1.75	1.7	2.11	1.85	1.58	1.54
	8	2.13	1.94	1.7	1.66	2.06	1.81	1.55	1.49
	10	2.1	1.9	1.69	1.62	1.97	1.78	1.52	1.45
Mixed system	0	2.85	2.48	2.41	2.35	2.81	2.45	2.39	2.33
	2	2.7	2.32	2.28	2.23	2.64	2.28	2.23	2.15
	4	2.62	2.26	2.2	2.14	2.54	2.22	2.13	2.06
	6	2.57	2.2	2.13	2.09	2.45	2.15	2.06	2.02
	8	2.52	2.18	2.08	2.02	2.43	2.12	2	1.98
	10	2.49	2.15	2.04	1.96	2.41	2.06	1.96	1.91

Table 3 Mole percent uptake of aliphatic penetrant of EPDM/SBR-SiO_2 composites with and without TESPT

Crosslinking system types	Nanosilica loading	Mole percent uptake (mol%) of aliphatic penetrant							
		Without TESPT				With TESPT			
		n-pentane	n-hexane	n-heptane	n-octane	n-pentane	n-hexane	n-heptane	n-octane
Sulphur system	0	2.42	2.34	2.28	2.24	2.39	2.31	2.25	2.21
	2	2.36	2.17	2.04	2.08	2.29	2.09	1.97	1.91
	4	2.18	2	1.87	1.84	2.04	1.92	1.82	1.77
	6	1.96	1.84	1.76	1.72	1.84	1.75	1.68	1.63
	8	1.9	1.8	1.7	1.64	1.81	1.71	1.6	1.58
	10	1.84	1.72	1.66	1.6	1.79	1.68	1.58	1.54
Peroxide system	0	1.95	1.9	1.84	1.81	1.92	1.87	1.81	1.79
	2	1.75	1.72	1.7	1.67	1.64	1.6	1.54	1.62
	4	1.69	1.64	1.58	1.54	1.53	1.5	1.47	1.43
	6	1.65	1.6	1.55	1.48	1.46	1.42	1.37	1.33
	8	1.61	1.55	1.5	1.44	1.41	1.39	1.35	1.3
	10	1.6	1.53	1.48	1.4	1.35	1.33	1.29	1.24
Mixed system	0	2.32	2.26	2.18	2.14	2.3	2.23	2.15	2.1
	2	2.25	2.15	2.06	1.96	2.17	2.11	1.99	1.9
	4	2.21	2.09	2	1.87	2.14	2.03	1.94	1.83
	6	2.17	2.04	1.95	1.82	2.09	1.97	1.91	1.8
	8	2.14	2.01	1.92	1.75	2.03	1.93	1.85	1.71
	10	2.09	1.97	1.9	1.72	2	1.9	1.82	1.69

Table 4 Mole percent uptake of chlorinated penetrant of EPDM/SBR-SiO_2 composites with and without TESPT

Crosslinking system types	Nanosilica loading	Mole percent uptake (mol%) of chlorinated penetrant					
		With TESPT			Without TESPT		
		Dichloromethane	Chloroform	Carbon tetrachloride	Dichloromethane	Chloroform	Carbon tetrachloride
Sulphur system	0	5.42	4.56	2.26	5.39	4.53	2.23
	2	5.1	4.28	2.03	5.04	4.13	1.96
	4	4.83	4	1.9	4.76	3.81	1.78
	6	4.6	3.83	1.81	4.52	3.66	1.73
	8	4.54	3.76	1.75	4.44	3.59	1.64
	10	4.5	3.72	1.71	4.35	3.55	1.61
Peroxide system	0	3.47	3.36	2.24	3.44	3.34	2.21
	2	3.3	3.14	2.11	3.17	3.04	2.04
	4	3.17	3.09	2.04	3.11	2.92	1.96
	6	3.13	3.06	2	3.06	2.83	1.9
	8	3.08	3	1.96	3.01	2.75	1.85
	10	3.02	2.96	1.92	2.96	2.67	1.81
Mixed system	0	3.8	3.42	2.29	3.77	3.39	2.26
	2	3.63	3.34	2.11	3.58	3.27	2.04
	4	3.55	3.28	2.03	3.5	3.21	1.96
	6	3.5	3.17	1.94	3.42	3.11	1.88
	8	3.45	3.12	1.9	3.38	3.05	1.84
	10	3.4	3.06	1.85	3.32	2.98	1.79

EPDM / SBR will meanwhile create a hydrogen bond with the silanol group of nanosilica.

3.4 Crosslinking Density

Crosslinking was the important phenomena required in most types of rubber materials in order to increase the mechanical strength and abrasion resistance. Under the vulcanizing temperature in the compressed mold set-up, most crosslinking reactions are done through hydraulic press. After the crosslinking process, the rubber network was described by crosslink density of the compound. The crosslinking density of the nanosilica-loaded EPDM/SBR composites with and without TESPT was

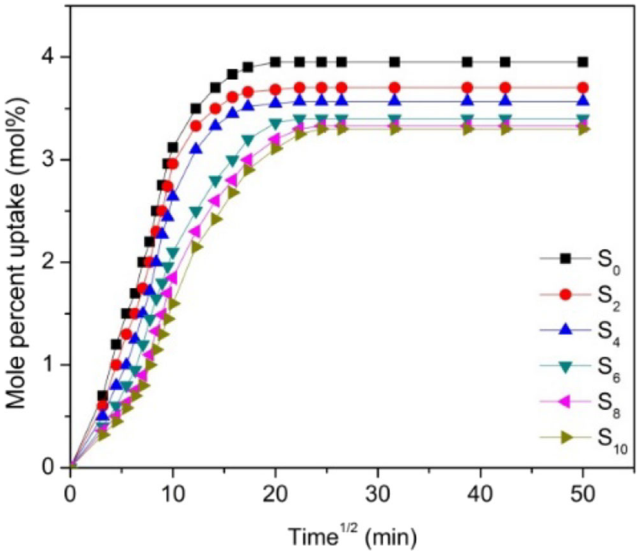

Fig. 13 Mole percent uptake of benzene by different nanosilica loading crosslinked with sulphur

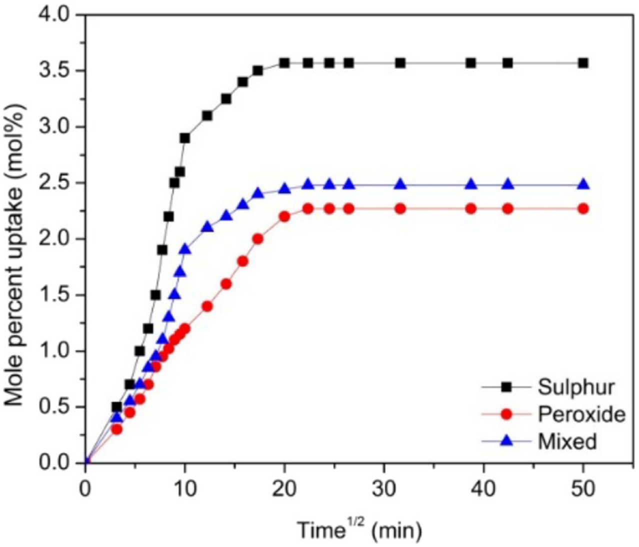

Fig. 14 Mole percent uptake of toluene through EPDM/SBR composites with different crosslinking systems

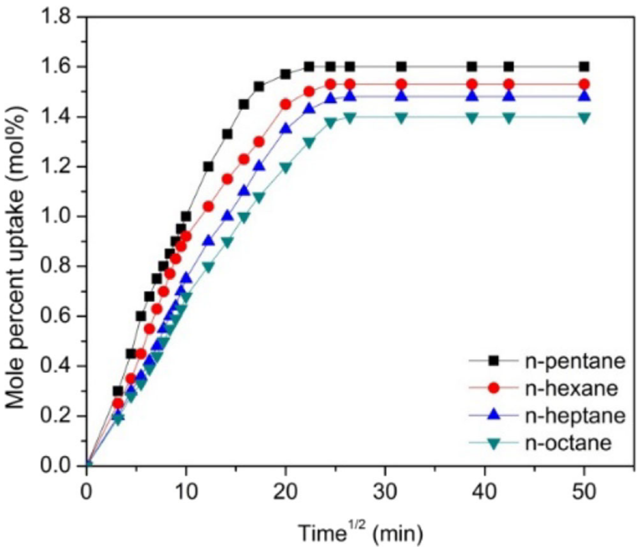

Fig. 15 Mole percent uptake of different aliphatic solvents through peroxide crosslinked 10 phr nanosilica filled EPDM/SBR composites

determined by solvent swelling method using Flory-Rehner equation and the experimental values of the crosslinking density are reported in Fig. 10. The rubber-filler interactions and chemical crosslinks are the important parameters that affect the crosslinking density of EPDM/SBR composites. Crosslinking density increases with increasing content of nanosilica which was due to better rubber-nanofiller interactions which results in better dispersion of nano materials at higher loading. Composite with TESPT shows a better improvement in crosslinking density as compared with the composites without TESPT. This indicates the silica nanoparticles in the composite without TESPT has a negative effect on curing which results in a lower crosslink density. With the TESPT, the crosslinking density of the composites increased considerably which indicates the effect of nanoparticles to restrict the rubber chains when they are attached to the nanoparticles through the TESPT. Higher crosslinking density of composites with TESPT indicates more strain on the EPDM/SBR-nanosilica network due to restricted chain mobility. Similar results are obtained from this kind of research work [24, 65]. The crosslinking density was highest for peroxide cured composite and lowest for sulphur cured composite among the various crosslinking systems for given nanosilica loading.

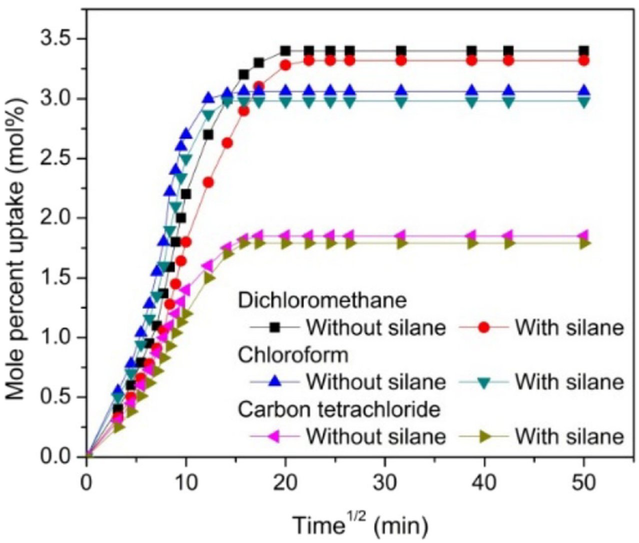

Fig. 16 Mole percent uptake of chlorinated solvents through 10 phr nanosilica filled EPDM/SBR composite with and without TESPT

3.5 Rebound Resilience

Figure 17 showed the effect of nanosilica loading and TESPT on the resistance of the EPDM / SBR composites to the rebound. The EPDM/SBR composites show similar trends as above; rubber composites' rebound resilience decreases with an increase in nanosilica concentration. The decreasing trend observed in the composite was due to better EPDM/SBR-nanosilica interaction. When more silica nanoparticles are introduced into the EPDM/SBR, the rubber chains elasticity has been reduced which results in lower resistance to the rebound [66]. It was clear that at a similar composite ratio, the rebound resilience of nanosilica filled EPDM/SBR composites with TESPT was found to be higher than the composite without TESPT. The surface property of the filler material plays a vital aspect in indicating the extent of EPDM/SBR-nanosilica interaction. The incorporation of particulate fillers into rubber materials leads to an improvement in hardness and a reduction in rebound resilience, particularly with high concentration of filler. Hence the composites with the same composition and crosslinked with sulphur always show higher values of rebound resilience than those crosslinked with the peroxide cured system, due to the structure of crosslinks and higher crosslink degree. The TESPT was also efficient in composites crosslinked with sulphur. While the presence of TESPT reduces the rebound resilience of both sulphur and peroxide crosslinked systems, the best rebound resilience was achieved with the sulphur system, as shown in Fig. 17.

3.6 Abrasion Resistance

The abrasion resistance was defined as its ability to withstand the progressive removal of rubber material from it surface as the consequence of mechanical action of a scraping, erosive, or rubbing nature [67]. Figure 18 indicated the volume loss of the

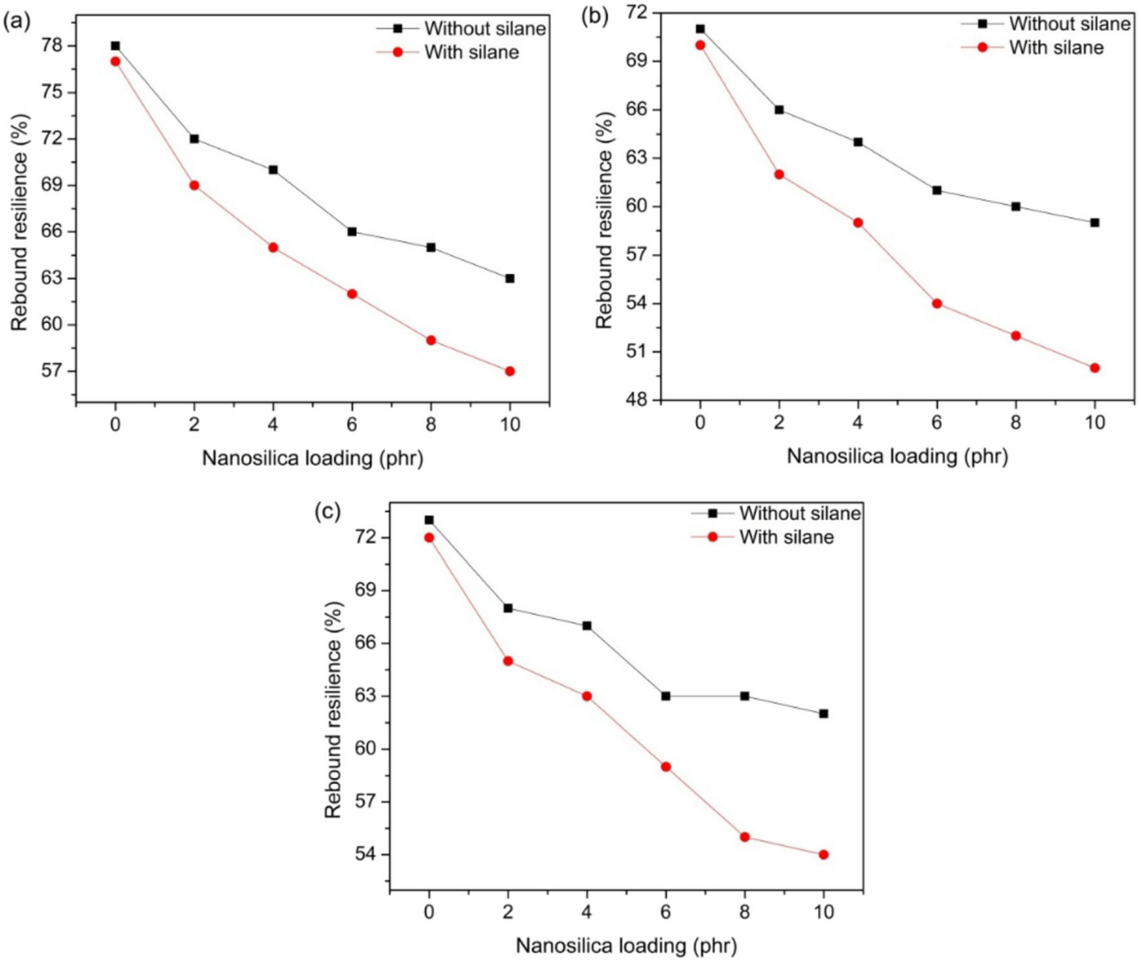

Fig. 17 Rebound resilience of the EPDM/SBR composites: **a** Sulphur cured composite, **b** Peroxide cured composite and **c** Mixed system cured composite

EPDM/SBR composites. The incorporation of nanosilica significantly reduced the abrasion ratio of EPDM / SBR composites. Generally, the abrasion loss and abrasion resistance are inversely related. With increasing nanosilica content, the abrasion resistance increased for all the different crosslinking systems. An increase in the nanosilica composition of the rubber composite reduces the loss of abrasion in the composites. This improvement was mainly due to the greater nanosilica surface area and better interfacial adhesion between filler and rubber [68]. In addition, nanoparticles show their greater interface between nanosilica and EPDM / SBR matrix and thus give better resistance to abrasion and adhesion compared to coarse ones.

3.7 Compression Set

The compression set was a test of the rubber composite's ability to sustain its elastic properties under the specified condition (i.e. time and temperature) after a long stress at a constant strain rate [8]. The compression set of the different crosslinking systems cured EPDM/SBR-SiO_2 composites with and without TESPT measured at 23 °C for 24 h and are tabulated in Table 5. The Table 5, clearly shows the value of compression set against nanosilica loading for EPDM/SBR compounds. From the table it was obvious that the compression set is low in the case of peroxide cured pure blends (EPDM / SBR), but as the nanosilica content increases, the compression set increases. The trend seems to be similar for both sulphur and mixed cured composites as discussed. Sulphur > mixed > peroxide was the compression set order followed for various crosslinking systems. This was due the fact that the increase in the concentration of nanosilica loading increases the crosslinking density of composite which in turn decreases the mobility of the polymeric chain. Thus induces stiffness in the EPDM/SBR-SiO_2 composite. The addition of

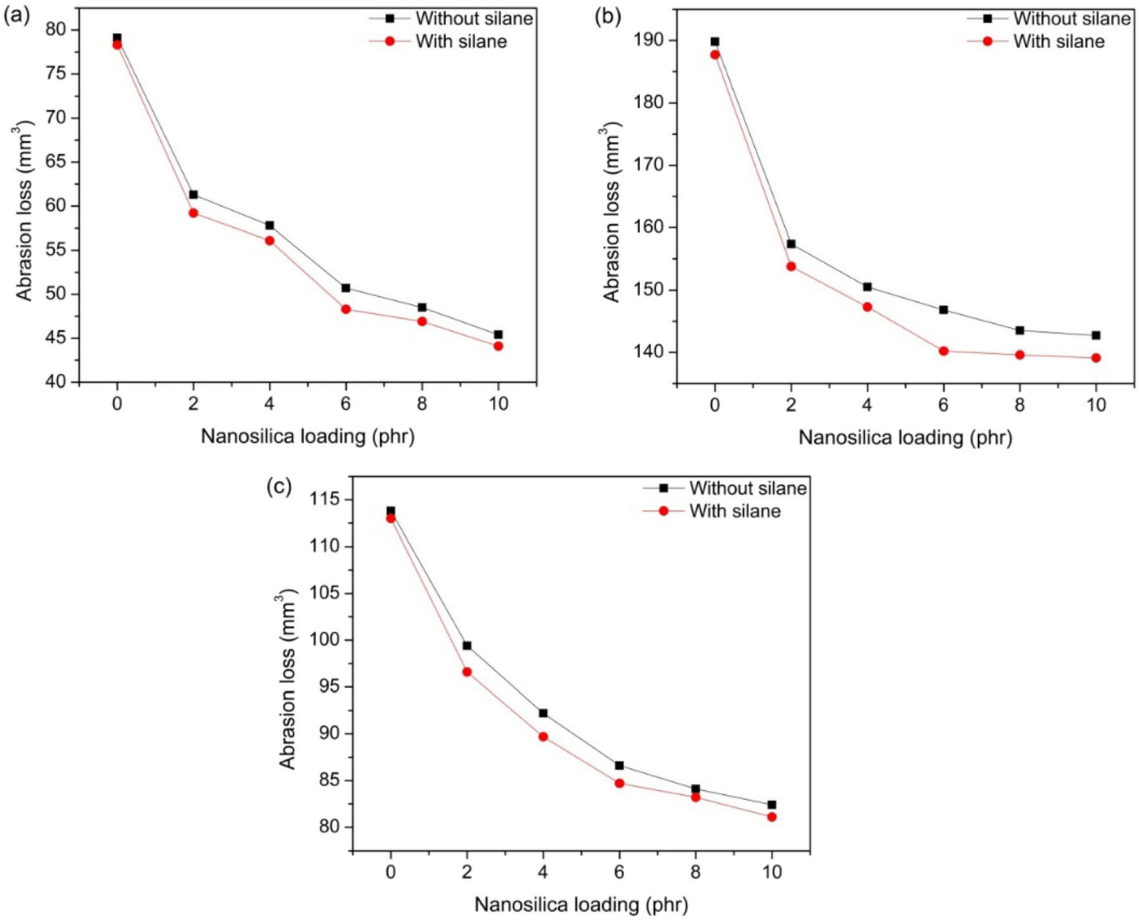

Fig. 18 Abrassion loss of the EPDM/SBR composites: **a** Sulphur cured composite, **b** Peroxide cured composite and **c** Mixed system cured composite

TESPT has increased the compression set of nanosilica filled EPDM/SBR composites for different crosslinking systems. When using TESPT a strong Si-O - Si bond was formed between the surface of the silane and the surface of the silica nanoparticle. Moreover, the composites of EPDM/SBR with and without TESPT were aged under compression load at 23 °C for 3 days. Table 5 presents the compression set of all EPDM/SBR composites with increasing ageing time. The compression set with time offered two stages: in the first stage (I: $0 < \text{time} \leq 2$ d), all composites had an increase in compression set. In the second stage (II: $\text{time} > 2$ d), the compression set of all composites showed a relatively increase. After ageing for 3 days, the compression set of sulphur, peroxide and mixed system cured composites with TESPT were 220%, 203% and 208% increase, respectively. From the Table 5, compression set of all EPDM/SBR composites with increasing ageing temperature. The compression set with temperature presented two stages: in the first stage (I: 23 °C < temperature ≤ 70 °C), all composites showed a drastic increase. In the second stage (II: 70 °C < temperature ≤ 100 °C), the compression set of all composites showed a slightly increase. The set of compressions also increases as the temperature increases. From the observation, it was clear that the temperature have a major influence on the compression set property of the composite. The lower range of compressions confirms the composite's retainable elastic property to the better. The compression set of sulfur, peroxide and mixed system cured composites with TESPT increased to 511%, 304% and 281% respectively after ageing at 100 °C.

3.8 Morphology

Figure 19 displays the FESEM micrographs of the composites of the EPDM/ SBR tensile broken surfaces along with the position of the tensile. Figure 19 (a, b), (c, d), (e, f) shows the surface morphology with the addition of 6 phr of nanosilica particles filled sulphur, peroxide and mixed system cured rubber composites with and without the presence TESPT, respectively. Similar to the other compounds, the compounds with TESPT exhibit

Table 5 Compression set for EPDM/SBR-SiO_2 composites

Nanosilica loading	Crosslinking system types	Compression set (%)									
		Without TESPT					With TESPT				
		For 1 day at 23 °C	For 2 day at 23 °C	For 3 day at 23 °C	For 1 day at 70 °C	For 1 day at 100 °C	For 1 day at 23 °C	For 2 day at 23 °C	For 3 day at 23 °C	For 1 day at 70 °C	For 1 day at 100 °C
0	Sulphur system	4.1	9.74	13.14	21.67	25.23	4.18	9.83	13.36	21.89	25.54
2		5.75	11.45	15.76	24.32	29.32	6.08	12.68	16.89	25.17	30.94
4		6.06	11.69	16.17	26.78	30.67	6.55	11.94	17.56	28.45	32.34
6		6.5	12.55	16.64	29.45	31.76	7.03	13.76	18.07	31.65	33.81
8		6.67	12.93	17.06	30.05	32.54	7.16	14.05	18.73	33.39	34.34
10		6.79	13.34	17.18	30.21	32.84	7.22	14.28	19.12	33.58	34.93
0	Peroxide system	1.97	4.63	6.18	7.56	8.29	2.08	4.78	6.31	7.78	8.41
2		2.6	6.34	8.45	9.32	11.46	3.2	7.18	9.76	10.54	12.73
4		2.76	6.58	8.97	10.45	12.71	3.28	7.67	10.1	11.67	13.45
6		2.97	6.87	9.23	12.87	13.37	3.5	8.03	10.56	14.62	15.94
8		3.1	7.15	9.45	13.74	15.56	3.7	8.17	10.93	15.07	17.52
10		3.17	7.28	9.78	13.95	16.73	3.91	8.23	11.09	15.43	18.04
0	Mixed system	2.89	6.85	9.12	10.78	11.38	3	6.98	9.25	11.03	11.42
2		3.56	9.04	11.34	13.63	15.27	4.18	9.71	12.79	14.74	16.52
4		3.78	9.38	11.72	14.56	17.76	4.96	10.85	13.67	15.63	18.66
6		3.93	9.89	12.56	16.98	18.89	5.71	11.56	14.61	17.81	20.44
8		4.06	10.45	12.78	17.34	19.76	6.07	12.89	15.87	18.69	21.79
10		4.19	10.9	12.95	17.86	20.67	6.23	13.31	16.43	18.95	22.41

very rougher morphology, tortuous broken surface and many tear-lines. The several lines of tears indicate the more energy needed to destroy the specimens. It is because of the strong nanosilica particle interactions with the matrix EPDM / SBR. In particularly Fig. 19 (b) show irregular rough surface with homogeneous dispersion and undulations of nanosilica particles. This indicates effective stress transfer and leads to the improvement in overall properties of EPDM/SBR with 6 phr nanosilica and TESPT composite. Figure 19 (g, h, i) indicates aggregated nanosilica fillers developed stress concentration points in the polymer matrix which leads to reduction in properties of the EPDM/SBR composites. In the composites filled with 10 phr of nanosilica and with TESPT the flat broken-out section morphology is indicative of reduced interfacial adhesion between rubber matrix and nanosilica particles, as can be presented in Fig. 19 (g, h, i).

4 Conclusions

The effect of nanosilica and crosslinking systems on cure characteristics, mechanical characteristics, swelling resistant, compression set, rebound resilience and wear (abrasion) resistance of EPDM / SBR composites with and without TESPT has been investigated in the current research.

1. From the analysis, it was apparent that the minimum torque, maximum torque, delta torque and cure rate index of EPDM / SBR composites with different curing agents, with and without TESPT, were observed to steps up with an increase in nanosilica concentration, whereas the scorching time and optimum cure time are decreased.
2. The introduction of nanosilica into the rubber compounds slowly increases the tensile strength, 100% modulus and the elongation at break. But, when the nanosilica loading exceeds 6 phr, further the addition of reinforcement in the matrix was found to be insignificant. This was due to the agglomeration of the nanoparticles in the composite and the reduced interfacial bonding between nanosilica particle and the matrix rubber blend material which was apparent from FESEM micrographs.
3. There were noticeable improvements in hardness, tear strength, abrasion and swelling resistance. Above mentioned properties showed higher for composites with TESPT compared to composites

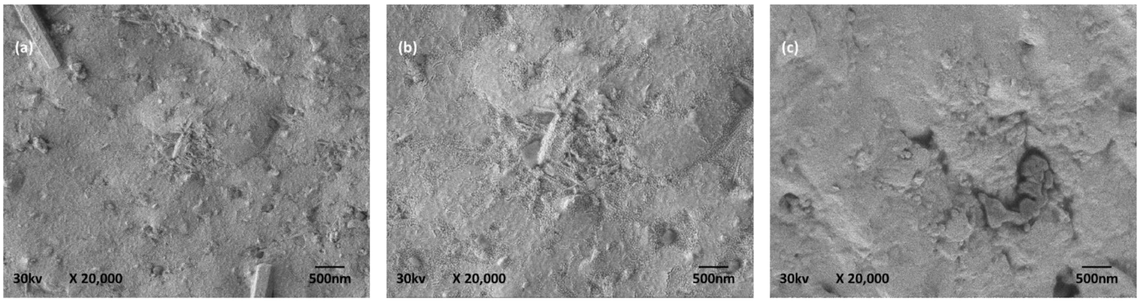

a) Sulphur cured EPDM/SBR blend reinforced with 6 phr of nanosilica (S$_6$)

b) Sulphur cured EPDM/SBR blend reinforced with 6 phr of nanosilica with TESPT (ST$_6$)

c) Peroxide cured EPDM/SBR blend reinforced with 6 phr of nanosilica (P$_6$)

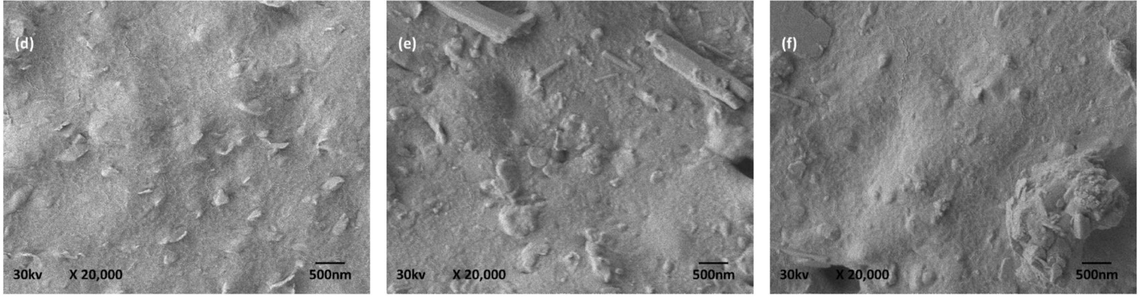

d) Peroxide cured EPDM/SBR blend reinforced with 6 phr of nanosilica with TESPT (PT$_6$)

e) Mixed system cured EPDM/SBR blend reinforced with 6 phr of nanosilica (M$_6$)

f) Mixed system cured EPDM/SBR blend reinforced with 6 phr of nanosilica with TESPT (MT$_6$)

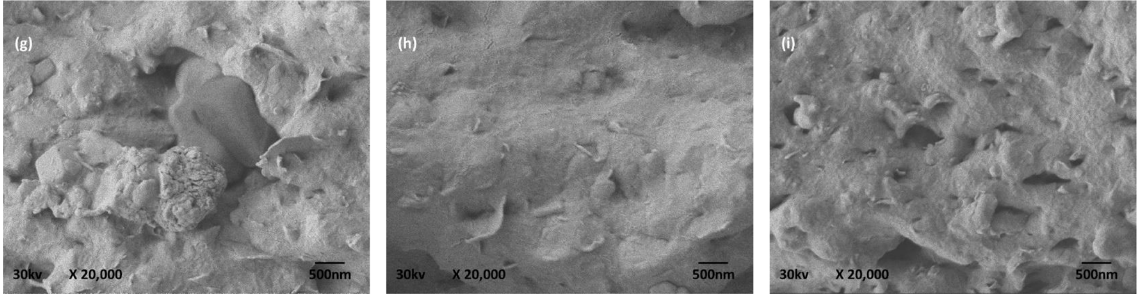

g) Sulphur cured EPDM/SBR blend reinforced with 10 phr of nanosilica with TESPT (ST$_{10}$)

h) Peroxide cured EPDM/SBR blend reinforced with 10 phr of nanosilica with TESPT (PT$_{10}$)

g) Mixed system cured EPDM/SBR blend reinforced with 10 phr of nanosilica with TESPT (MT$_{10}$)

Fig. 19 The tensile fractured surfaces with magnification X = 20,000 of nanosilica filled EPDM/SBR composites: **a** S$_6$, **b** ST$_6$, **c** P$_6$, **d** PT$_6$, **e** M$_6$, **f** MT$_6$, **g** ST$_{10}$, **h** PT$_{10}$ and **i** MT$_{10}$

without TESPT. This improvement in the properties indicates stronger filler-rubber matrix interfacial adhesion and proper wetting of silica nanoparticles.

4. Among three crosslinking systems used, sulphur cured EPDM/SBR composites with TESPT show best mechanical properties, swelling and abrasion resistance.
5. Owing to the TESPT can form physical and chemical effects with nanosilica particles, and the chemical interface between nanosilica and rubber matrix constructed by TESPT. Therefore, TESPT can greatly improve the dispersion of nanosilica particles in EPDM/SBR composites.
6. These noticeable improvements in overall properties by the use of TESPT in nanosilica filled composites, may open up new opening for the preparation of environmental friendly rubber materials as well as high performance materials.

References

1. Arroyo M, Lopez-Manchado MA, Herrero B (2003) Organo-montmorilloniteas substitute of carbon black in natural rubber compounds. Polymer 44:2447–2453
2. Vishvanathperumal S, Gopalakannan S (2017) Swelling properties, compression set behavior and abrasion resistance of ethylene-propylene-diene rubber/styrene butadiene rubber blend Nanocomposites. Polymer Korea 41:433–442
3. Nugay N, Erman B (2001) Property optimization in nitrile rubber composites via hybrid filler systems. J Appl Polym Sci 79:366–371
4. Vishvanathperumal S, Gopalakannan S (2016) Reinforcement of ethylene vinyl acetate with carbon black/silica hybrid filler composites. Appl Mech Mater 852:16–22
5. Senthilvel K, Vishvanathperumal S, Prabu B, John Baruch L (2016) Studies on the morphology, cure characteristics and mechanical properties of acrylonitrile butadiene rubber with hybrid filler (carbon black / silica) composite. Polym Polym Compos 24: 473–480
6. Lu YL, Li Z, Yu ZZ, Tian M, Zhang LQ, Mai YW (2007) Microstructureand properties of highly filled rubber/clay nanocomposites prepared by melt blending. Compos Sci Technol 67:2903–2913
7. Usuki A, Kawasumi M, Kojima Y, Okada A, Kurauchi T, Kamigaito O (1993) Swelling behavior of montmorillonite cation exchanged for ω-amino acids by 3-caprolactam. J Mater Res 8: 1174–1178
8. Vishvanathperumal S, Navaneethakrishnan V, Gopalakannan S (2018) The effect of Nanoclay and hybrid filler on curing characteristics, mechanical properties and swelling resistance of ethylene vinyl acetate/styrene butadiene rubber blend composite. J Adv Microsc Res 13:469–476
9. Shanmugharaj AM, Bae JH, Lee KY, Noh WH, Lee SH, Ryu SH (2007) Physical and chemical characteristics of multiwalled carbon nanotubes functionalized with aminosilane and its influence on the properties of natural rubber composites. Compos Sci Technol 67: 1813–1822
10. Karami Z, Jazani OM, Navarchian AH, Karrabi M, Vahabi H, Saeb MR (2019) Well-cured silicone/halloysite nanotubes nanocomposite coatings. Progress in Organic Coatings 129:357–365
11. Vaibhav V, Vijayalakshmi U, Mohana Roopan S (2015) Agricultural waste as a source for the production of silica nanoparticles. Spectrochim Acta A Mol Biomol Spectrosc 139:515–520
12. Dong B, Liu C, Wu YP (2014) Fracture and fatigue of silica/carbon black/natural rubber composites. Polym Test 38:40–45
13. Liu X, Zhao S, Zhang X, Li X, Bai Y (2014) Preparation, structure, and properties of solution-polymerized styrene-butadiene rubber with functionalized end-groups and its silica-filled composites. Polymer (Guildf) 55:1964–1976
14. Saeed F, Ansarifar A, Ellis RJ, Meskel YH, Irfan MS (2012) Two advanced styrene butadiene/polybutadiene rubber blends filled with a silanized silica nanofiller for potential use in passenger car tire tread compound. J Appl Polym Sci 123:1518–1529
15. Hilonga A, Kim JK, Sarawade PB, Quang DV, Shao GN, Elineema G, Kim HT (2012) Synthesis of mesoporous silica with superior properties suitable for green tire. J Ind Eng Chem 18:1841–1844
16. Lin Y, Liu S, Peng J, Liu L (2016) The filler-rubber interface and reinforcement in styrene butadiene rubber composites with graphene/silica hybrids: a quantitative correlation with the constrained region. Compos Appl Sci Manuf 86:19–30
17. Hassan AA, Wang S, Anwar F (2019) Physiochemical characterization of soybean oil derived silanized factice and its interaction with styrene butadiene rubber/silica composite. Polym Test 78: 105933
18. Li Y, Han B, Liu L, Zhang F, Zhang L, Wen S, Lu Y, Yang H, Shen J (2013) Surface modification of silica by two-step method and properties of solution styrene butadiene rubber (SSBR) nanocomposites filled with modified silica. Compos Sci Technol 88:69–75
19. Gui Y, Zheng J, Ye X, Han D, Xi M, Zhang L (2016) Preparation and performance of silica/SBR master batches with high silica loading by latex compounding method. Compos B Eng 85:130–139
20. Bertora A, Castellano M, Marsano E, Alessi M, Conzatti L, Stagnaro P, Colucci G, Priola A, Turturro A (2011) A new modifier for silica in reinforcing SBR elastomers for the Tyre industry. Macromol Mater Eng 296:455–464
21. Jiang F, Zhang X, Hwang W, Briber RM, Fang Y, Wang H (2019) Supramolecular luminescent triblock copolymer thermoplastic elastomer via metal-ligand coordination. Polym Test 78:105956
22. Byer JT, Wagner MP (1999) Fillers. In Rubber Technology. M. Morton, Ed. Springer Science Business Media, Dordrecht, the Netherlands. p.97
23. Xiao Y, Zou H, Zhang L, Ye X, Han D (2020) Surface modification of silica nanoparticles by a polyoxyethylene sorbitan and silane coupling agent to prepare high-performance rubber composites. Polym Test 81:106195
24. Dileep P, Narayanankutty SK (2020) Styrenated phenol modified nanosilica for improved thermo-oxidative and mechanical properties of natural rubber. Polym Test 82:106302
25. J.W.ten Brinke, Debnath SC, Reuvekamp LAEMK, Noordermeer JWM (2003) Mechanistic aspects of the role of coupling agents in silica-rubber composites. Compos Sci Technol, 63
26. Goerl U, Hunsche A, Mueller A, Koban HG (1997) Investigations into the silica/silane reaction system. Rubber Chem Technol 70: 608–623
27. Kaewsakul W, Sahakaro K, Dierkes WK, Noordermeer JWM (2012) Optimization of mixing conditions for silica-reinforced natural rubber tire tread compounds. Rubber Chem Technol 85:277–294
28. Reuvekamp LAEM, J.W.ten Brinke, P.J.van Swaaij, Noordermeer JWM (2002) Effects of mixing conditions-reaction of TESPT silane coupling agent during mixing with silica filler and tire rubber, Kautschuk Gummi Kunststoffe, 55
29. Hayichelaeh C, Reuvekamp LAEM, Dierkes WK, Blume A, Noordermeer JWM, Sahakaro K (2017) Reinforcement of natural rubber by silica/silane in dependence of different amines. Rubber Chem Technol 90:651–666
30. Hayichelaeh C, Reuvekamp LAEM, Dierkes WK, Blume A, Noordermeer JWM, Sahakaro K (2018) Promoting interfacial compatibility of silica-reinforced natural rubber tire compounds by aliphatic amine. Rubber Chem Technol 91:433–452
31. Zhong B, Zeng X, Chen W, Luo Q, Hu D, Jia Z, Jia D (2019) Nonsolvent-assisted surface modification of silica by silane and antioxidant for rubber reinforcement. Polym Test 78:105949
32. Zheng J, Han D, Ye X, Wu X, Wu Y, Wang Y, Zhang L (2018) Chemical and physical interaction between silane coupling agent with long arms and silica and its effect on silica/natural rubber composites. Polymer (Guildf) 135:200–210
33. Das S, Chattopadhyay S, Dhanania S, Bhowmick AK (2019) Reactive grafting of 3-octanoylthio-1-propyltriethoxysilane in styrene butadiene rubber: characterization and its effect on silica reinforced tire composites. Polymer 179:121693
34. Nakamura Y, Honda H, Harada A, Fujii S, Nagata K (2009) Mechanical properties of silane-treated, silica-particle-filled polyisoprene rubber composites: effects of the loading amount and alkoxy group numbers of a silane coupling agent containing mercapto groups. J Appl Polym Sci 113:1507–1514
35. Seo G, Park SM, Ha K, Choi KT, Hong CK, Kaang S (2010) Effectively reinforcing roles of the networked silica prepared using 3,30 -bis(triethoxysilylpropyl)tetrasulfide in the physical properties of SBR compounds. J Mater Sci 45:1897–1903

36. Reuvekamp LAEM, J.W.ten brinke, van Swaaij PJ, Noordermeer JWM (2002) Effects of time and temperature on the reaction of tespt silane coupling agent during mixing with silica filler and tire rubber. Rubber Chem Technol 75:187–198
37. Ramier J, Chazeau L, Gauthier C, Guy L, Bouchereau MN (2007) Influence of silica and its different surface treatments on the vulcanization process of silica filled SBR. Rubber Chem Technol 80: 183–193
38. Tang Z, Huang J, Wu X, Guo B, Zhang L, Liu F (2015) Interface engineering toward promoting Silanization by ionic liquid for high-performance rubber/silica composites. Ind Eng Chem Res 54: 10747–10756
39. Soo-Jin P, Ki-Sook C (2003) Filler–elastomer interactions: influence of silane coupling agent on crosslink density and thermal stability of silica/rubber composites. J Colloid Interface Sci 267: 86–91
40. Changjie Y, Qiuyu Z, Junwei G, Jucheng Z, Guangbi G, Tao L, Hepeng Z (2013) In situ silica reinforcement of vinyltriethoxysilane-grafted styrene–butadiene rubber by sol–gel process. J Appl Polym Sci 128:2262–2268
41. Cartasegna S (1986) Silane-grafted/moisture-curable Ethyle-propylene elastomers for the cable industry, presented at the meeting of the American Chemical Society, New York, April 8–11
42. Nakamura N, Hayashi H (2010) The influence of the degree of Silane coupling agents - polymers interaction on the viscoelastic properties. Int Polym SciTechnol 37:167–173
43. Sen AK, Mukherjee B, Bhattacharya AS, De PP, Bhowmick Ak (1992) Kinetics of silane grafting and moisture crosslinking of polyethylene and ethylene propylene rubber. J Appl Polym Sci 44:1153
44. Datta RN, Flexsys BV (2002) Rubber curing systems. Rapra Review Reports 12(12):5–30
45. Monfared A, Jalali-Arani A, Mohammadi N (2014) The effect of epoxidized natural rubber and two kinds of organoclay upon molecular interaction, structure and mechanical properties of (styrene–butadiene rubber/acrylonitrile-butadiene rubber/organoclay) nanocomposites. J Macromol Sci Part B 53(5):918–930
46. Dubey KA, Bhardwaj YK, Chaudhari CV, Bhattacharya S, Gupta SK, Sabharwal S (2006) Radiation effects on SBR–EPDM blends: a correlation with blend morphology. J Polym Sci B Polym Phys 44(12):1676–1689
47. Zanchet A, Carli LN, Giovanela M, Brandalise RN, Crespo JS (2012) Use of styrene butadiene rubber industrial waste devulcanized by microwave in rubber composites for automotive application. Mater Des 39:437–443
48. Muraleedharan Nair T, Kumaran MG, Unnikrishnan G (2004) Mechanical and aging properties of cross-linked ethylene propylene Diene rubber / styrene butadiene rubber blends. J Appl Polym Sci 93:2606–2621
49. Vishvanathperumal S, Gopalakannan S (2019) Effects of the Nanoclay and crosslinking systems on the mechanical properties of ethylene-propylene-diene monomer/styrene butadiene rubber blends Nanocomposite. Silicon 11:117–135
50. Vishvanathperumal S, Anand G (2020) Effect of Nanoclay/ Nanosilica on the mechanical properties. Abrasion and Swelling Resistance of EPDM/SBR Composites, Silicon 12:1925–1941
51. Sun Y, He J, Zhong B, Zhu L, Liu F (2019) A synthesized multi-functional rubber additive and its improvements on the curing and antioxidative properties of styrene-butadiene rubber/silica composites. Polym Degrad Stab 170:108999
52. Vishvanathperumal S, Navaneethakrishnan V, Anand G, Gopalakannan S (2020) Evaluation of crosslink density using material constants of ethylene-propylene-Diene monomer/styrene-butadiene rubber with different Nanoclay loading: finite element analysis-simulation and experimental. Advanced Science, Engineering and Medicine 12:632–642
53. Manoj KC, Kumari P, Rajesh C, Unnikrishnan G (2010) Aromatic liquid transport through filled EPDM/NBR blends. J Polym Res 17: 1–9
54. Sujith A, Unnikrishnan G (2006) Molecular sorption by heterogeneous natural rubber/poly(ethylene-co-vinyl acetate) blend systems. J Polym Res 13:171–180
55. Thomas PC, Tomlal JE, Selvin TP, Thomas S, Joseph K (2010) High-performance nanocomposites based on acrylonitrile butadiene rubber with fillers of different particle size: Mechanical and morphological studies. Polymer Composites 31:1515–1524
56. Flory PJ, Rehner J (1943). Statistical mechanics of cross-linked polymer networks I rubber like elasticity J Chem Phys 11:512
57. Naseri ASZ, Arani AJ (2015) A comparison between the effects of gamma radiation and sulfur cure system on the microstructure and crosslink network of (styrene butadiene rubber/ethylene propylene diene monomer) blends in presence of nanoclay. Radiat Phys Chem 115:68–74
58. Noriman NZ, Ismail H (2012) Properties of styrene butadiene rubber (SBR)/recycled acrylonitrile butadiene rubber (NBRr) blends: the effects of carbon black/silica (CB/silica) hybrid filler and silane coupling agent, Si69. J Appl Polym Sci 124:19–27
59. Zhang C, Tang Z, Guo B, Zhang L (2018) Significantly improved rubber-silica interface via subtly controlling surface chemistry of silica. Compos Sci Technol 156
60. Kong L, Li F, Wang F, Miao Y, Huang X, Zhu H, Lu Y (2018) In situ assembly of SiO_2 nanodots/layered double hydroxide nanocomposite for the reinforcement of solution-polymerized butadiene styrene rubber/butadiene rubber. Compos Sci Technol 158:9–18
61. Prasertsri S, Rattanasom N (2012) Fumed and precipitated silica reinforced natural rubber composites prepared from latex system: mechanical and dynamic properties. Polym Test 31:593–605
62. Wu X (2019) Junchi Zheng, Bingyong Han, Liqun Zhang, Jianmin Lu, Xin Ye, designing novel epoxy-terminated polybutadiene to construct chemical interface between nanosilica and rubbers with green nature. Compos Part B 178:107451
63. Padmini M, Radhakrishnan CK, Sujith A, Unnikrishnan G, Purushothaman E (2006) Molecular transport of aliphatic hydrocarbons through styrene butadiene rubber/ethylene vinyl acetate blends. J Appl Polym Sci 101:2884–2897
64. Unnikrishnan G, Thomas S (1998) Interaction of crosslinked natural rubber with chlorinated hydrocarbons. Polymer 39:3933–3938
65. Yan N, Wu JK, Zhan YH, Xia HS (2009) Carbon nanotubes/carbon black synergistic reinforced natural rubber composites. Plast Rubber Compos 38:290–296
66. Arayapranee W, Garry LR (2008) A comparative study of the cure characteristics, processability, mechanical properties, ageing, and morphology of rice husk ash, silica and carbon black filled 75: 25 NR/EPDM blends. J Appl Polym Sci 109:932–941
67. Durandish M, Alipourb A (2013) Investigation into morphology, microstructure and properties of SBR/EPDM/ organomontmorillonite nanocomposites. Chin J Polym Sci 31(4): 660–669
68. Alipour A, Naderi G, Bakhshandeh GR, Vali H, Shokoohi S (2011). Int Polym Proc 26:48